



Research article

Dynamical complexities and chaos control in a Ricker type predator-prey model with additive Allee effect

Vinoth Seralan¹, R. Vadivel², Dimplekumar Chalishajar^{3,*} and Nallappan Gunasekaran⁴

¹ Centre for Nonlinear Systems, Chennai Institute of Technology, Chennai 600069, Tamil Nadu, India

² Department of Mathematics, Faculty of Science and Technology, Phuket Rajabhat University, Phuket 83000, Thailand

³ Department of Applied Mathematics, Virginia Military Institute (VMI), 435 Mallory Hall, Lexington, VA 24450, USA

⁴ Eastern Michigan Joint College of Engineering, Beibu Gulf University, Qinzhou 535011, China

* **Correspondence:** Email: chalishajardn@vmi.edu.

Abstract: This work investigates the dynamic complications of the Ricker type predator-prey model in the presence of the additive type Allee effect in the prey population. In the modeling of discrete-time models, Euler forward approximations and piecewise constant arguments are the most frequently used schemes. In Euler forward approximations, the model may undergo period-doubled orbits and invariant circle orbits, even while varying the step size. In this way, differential equations with piecewise constant arguments (Ricker-type models) are a better choice for the discretization of a continuous-time model because they do not involve any step size. First, the interaction between prey and predator in the form of the Holling-II type is considered. The essential mathematical features are discussed in terms of local stability and the bifurcation phenomenon as well. Next, we apply the center manifold theorem and normal form theory to achieve the existence and directions of flip bifurcation and Neimark-Sacker bifurcation. Moreover, this paper demonstrates that the outbreak of chaos can stabilize in the considered model with a higher value of the Allee parameter. The existence of chaotic orbits is verified with the help of a one-parameter bifurcation diagram and the largest Lyapunov exponents, respectively. Furthermore, different control methods are applied to control the bifurcation and fluctuating phenomena, i.e., state feedback, the Ott-Grebogi-Yorke, and hybrid control methods. Finally, to ensure our analytical results, numerical simulations have been carried out using MATLAB software.

Keywords: Allee effect; bifurcation; discrete system; largest Lyapunov exponent; local stability; predator-prey model

Mathematics Subject Classification: 92B05, 34C23, 34C25, 34D20, 39A28

1. Introduction

The intricate ecosystems found in the natural world are mostly the result of predator-prey interactions. Effective mathematical models are developed to address the problems in predator-prey interaction. A basic model for two species communities was formulated by Lotka in 1925 and Volterra in 1931. The predator's prey feeding rate is one essential component of predator-prey interaction. In literature, many interaction functions have been modeled, for example, Holling type I, type II or type III [1], ratio-dependent [2], Crowley-Martin [3] and Beddington-DeAngelis models [4, 5]. In recent years, the predator-prey model of Holling type II with different biological situations has been considered in the literature. For instance, in [6], the authors considered such a model with prey refuge and showed that the model parameters have crucial importance in the coexistence, stability and oscillation of their considered model. In reality, a predator consumes prey at different rates, depending on the species. Leslie and Gower [7] proposed a predator-prey model in which the predator's growth function is given by the ratio of the sizes of predator and prey. Differential equations describe the evolution of systems in continuous and discrete time. Further, discrete models are more realistic if the populations are small or if births and deaths occur at discrete times or within certain time intervals, such as a generation [8, 9].

To model real ecosystems, the term "Allee effect" is unavoidable and meaningful. Thus, many researchers have paid much attention to studying the dynamics of predator-prey models with the Allee effect [10, 11]. There are two types of Allee effects: weak and strong. In the weak Allee effect, for the low population size, the per capita growth rate is positive and there is no threshold to grow [12]. But, in the case of the strong Allee effect, the per capita growth is negative and there is a population threshold introduced by the Allee effect, so the population must surpass this threshold to grow [13]. The Allee effect can be introduced in different ways, namely, multiplicative [14] and additive [13]. Discrete-time predator-prey model with Allee effects was studied in [15, 16], and some more recent developments in predator-prey models can be found in [17–19]. Based on the above discussions, the Allee effect term is incorporated into prey growth for this study.

The study of stability analysis, bifurcation behavior, namely, flip bifurcation and Neimark-Sacker bifurcation, and control of the chaos of the discrete-time model has long been an issue of significant interest for researchers [20, 21]. Among the mathematics, physics and engineering communities, chaos control has been extensively studied [22], whereas the problem of controlling chaos in ecology has been given in [24]. In some nonlinear systems, there is a major route to chaos via period doubling. In [25], the authors proposed a new hybrid control method to control the chaotic orbits by using state feedback and parameter perturbation for the period-doubling bifurcation. The chaotic attractor can be converted into one of the possible attracting time-periodic motions by giving small perturbations to the system parameters [26]. Recently, the work related to controlling chaos in the predator-prey model has been of greater interest to researchers. For instance, a predator-prey model with the Allee effect and cannibalism in the discrete-time model has been found in the literature [27], where the authors showed that the considered system undergoes flip and Neimark-Sacker bifurcations. Further, they discussed the various methods to control the chaos. A discrete-time classical Lotka-Volterra model obtained by applying the method of a piecewise constant argument for differential equations has been proposed in [28]. The authors studied the stability, bifurcation and chaotic behavior of their proposed model. Also, they implemented hybrid control and the Ott-Grebogi-Yorke (OGY) method to control

bifurcation and chaotic behavior.

Since it was an interesting topic for the researchers, we are motivated by the above literature. To the best of our knowledge, the study of stability, bifurcation and chaos control analysis for a discrete-time prey-predator model with the additive Allee effect has not been studied. In this article, we aim to study the discrete-time Holling type II predator-prey model with the additive Allee effect in prey growth. The main highlights of this paper are listed as follows:

- 1) We use the method of piecewise constant arguments for the differential equations to obtain the discrete-time model. The model is a good representation of the populations' interaction, which has non-overlapping generations.
- 2) We study the impact of the Allee effect in terms of the existence and local stability properties of all positive equilibrium points of the discrete model.
- 3) We derive the conditions for the existence of flip and Neimark-Sacker bifurcations near the interior equilibrium point for the discrete model by taking the Allee parameter as a bifurcation parameter. Further, we discuss the properties of both bifurcations with the help of the center manifold (CM) theorem and normal form theory.
- 4) We utilize the state and OGY feedback and hybrid control methods to control the bifurcating and chaotic behavior of the discrete model. We provide extensive numerical simulations to show the rich dynamics, including periodic windows, invariant circles and chaos in the discrete model.

The rest of the article is arranged as follows: The discrete-time Holling type II predator-prey model with the additive type Allee effect is given, and the existence and local stability of equilibrium points are discussed in Section 2. Furthermore, an analysis of the model's dynamics is presented, including the identification of key parameters and their influence on the system's behavior. In Section 3, the bifurcation behavior of the proposed model is thoroughly examined. Two types of bifurcations, such as flip and Neimark-Sacker bifurcations, are investigated to gain a comprehensive understanding of the system's response to parameter changes. In Section 4, the state and OGY feedback and hybrid control techniques for the considered predator-prey model are discussed. The effectiveness of these control approaches is highlighted, emphasizing their ability to regulate and stabilize system dynamics. To ensure the validity and reliability of the mathematical results, extensive numerical simulations are presented in Section 5. Lastly, in Section 6, a comprehensive conclusion and a brief discussion are presented.

2. Model formation

First, we describe the continuous-time Holling type II prey-predator model with the additive Allee effect [29], as follows:

$$\begin{cases} \frac{dH(t)}{dt} = H(t) \left(r \left(1 - \frac{H(t)}{k} \right) - \frac{\alpha}{\beta + H(t)} - \frac{a_1 P(t)}{1 + a_1 a_2 H(t)} \right), \\ \frac{dP(t)}{dt} = P(t) \left(\frac{\gamma a_1 H(t)}{1 + a_1 a_2 H(t)} - d \right), \end{cases} \quad (2.1)$$

where $H(t)$ and $P(t)$ are the population sizes of prey and predator respectively at time t ; r and k represent the growth rate and carrying capacity of prey, respectively; γ and d represent the consumption rate of the predator on prey and per capita death rate of the predator, respectively. The most common type of

functional response is Holling type II, which is based on the idea that, if prey species is low, the rate of predation is proportional to prey density and is of the form $\frac{a_1 H(t)}{1+a_1 a_2 H(t)}$, where a_1 and a_2 represent the predator capture rate and handling time per prey, respectively.

In general, the term $\frac{\alpha}{\beta+H(t)}$ is known as the additive Allee effect, where α and β represent the severity of the Allee effect and the prey population size at which fitness is half of its maximum value, respectively. Many studies have been conducted to understand the dynamics of prey-predator system models with the additive Allee effect [30–32].

To reduce the complexity, and, for our convenience, after redefining the parameters, the model (2.1) takes the form

$$\begin{cases} \frac{dH(t)}{dt} = H(t) \left(a - bH(t) - \frac{\alpha}{\beta + H(t)} - \frac{cP(t)}{e + H(t)} \right), \\ \frac{dP(t)}{dt} = P(t) \left(\frac{fH(t)}{e + H(t)} - d \right), \end{cases} \quad (2.2)$$

where $H(t) \geq 0$, $P(t) \geq 0$, $a = r$, $b = \frac{r}{k}$, $c = \frac{a_1}{a_1 a_2}$, $e = \frac{1}{a_1 a_2}$ and $f = \frac{\gamma a_1}{a_1 a_2}$. Note that, in the sense of [33], if $\alpha < a\beta$ ($\alpha > a\beta$), the Allee effect is the weak (strong) one.

Next, based on the appropriate modification of overlapping generations, one can get the difference equations for modeling a population with non-overlapping generations. Euler approximations, non-standard finite difference schemes [34] and piecewise constant arguments [35,36] are the most common methods to obtain discrete versions from the continuous models. In this way, differential equations with piecewise constant arguments have been useful. Let us assume that the populations have no overlap between the successive generations and the population growth occurs in discrete steps $t \in [n, n+1)$, $n = 0, 1, 2, 3, \dots$. Also, consider that the variables and constants in (2.2) change in regular time intervals and incorporate this idea; then the corresponding discrete-time model for (2.2) is obtained by the method of piecewise constant arguments for differential equations, as follows:

$$\begin{cases} H(n+1) = H(n) \exp \left[a - bH(n) - \frac{\alpha}{\beta + H(n)} - \frac{cP(n)}{e + H(n)} \right], \\ P(n+1) = P(n) \exp \left[\frac{fH(n)}{e + H(n)} - d \right], \end{cases} \quad (2.3)$$

where $H(n+1)$ and $P(n+1)$ denote the populations in generation $n+1$ that are related to the sizes $H(n)$ and $P(n)$ of the populations in the preceding generation n and a, b, c, d, e, f, α and β are all positive constants.

Note, in the absence of a predator P and the Allee effect, the above model (2.3) becomes a one-dimensional model similar to the Ricker model [37], namely,

$$H(n+1) = H(n)e^{a-bH(n)}.$$

This system represents the relationship between the current and previous population size H . In a logistic map, the population's rate of per capita growth falls as the population size approaches a limit set by the availability of resources. On the Ricker map, population growth is almost exponential; however, as population size increases, the instantaneous growth rate declines linearly; and, eventually, population size reaches a plateau and oscillates around a mean.

The main aim of this paper is to study the local stability, bifurcation behavior and various chaos control analyses for the discrete time prey-predator model (2.3) with the additive Allee effect in the case of the weak one in $\mathbb{R} = \{(H, P) | H > 0, P > 0\}$.

2.1. Equilibria

We need to solve the following equations to find the equilibrium points of the model (2.3):

$$\begin{cases} a - bH - \frac{\alpha}{\beta + H} - \frac{cP}{e + H} = 0, \\ \frac{fH}{e + H} - d = 0. \end{cases} \quad (2.4)$$

By direct substitution, from (2.4), we have three positive equilibrium points: The trivial equilibrium point $(0, 0)$, the predator-free equilibrium point $(\bar{H}, 0)$, where \bar{H} is the positive root of the equation

$$b\bar{H}^2 + (b\beta - a)\bar{H} + \alpha - a\beta = 0, \quad (2.5)$$

and the interior equilibrium point (H^*, P^*) , which is given by

$$(H^*, P^*) = \left(\frac{de}{f-d}, \frac{(a - bH^*)(\beta + H^*)(e + H^*) - \alpha(e + H^*)}{c(\beta + H^*)} \right).$$

Then from [29], we have the following lemma.

Lemma 1. Consider $\alpha < a\beta$; then, the model (2.3) has a unique boundary equilibrium $(\bar{H}, 0) = \left(\frac{(a-b\beta) + \sqrt{(a-b\beta)^2 + 4b(a\beta + \alpha)}}{2b}, 0 \right)$. Also, the model (2.3) has a unique interior equilibrium $(H^*, P^*) = \left(\frac{de}{f-d}, \frac{(a-bH^*)(\beta+H^*)(e+H^*) - \alpha(e+H^*)}{c(\beta+H^*)} \right)$ if $\alpha < (a - bH^*)(\beta + H^*)$ and $\max\left(\beta, \frac{de}{f-d}\right) < \frac{a}{b} < \beta + \frac{de}{f-d}$.

2.2. Local stability analysis

Next, the Jacobian matrix for the model (2.3) at arbitrary equilibrium point (H, P) is calculated to investigate the local stability property:

$$J = \begin{bmatrix} \left(1 - bH + \frac{\alpha H}{(\beta + H)^2} + \frac{cHP}{(e + H)^2}\right)A_1 & -\left(\frac{cH}{e + H}\right)A_1 \\ \left(\frac{efP}{(e + H)^2}\right)A_2 & A_2 \end{bmatrix}, \quad (2.6)$$

where $A_1 = \exp\left(a - bH - \frac{\alpha}{\beta + H} - \frac{cP}{e + H}\right)$ and $A_2 = \exp\left(\frac{fH}{e + H} - d\right)$.

The Jacobian matrix of (2.3) derived at $(0, 0)$ is

$$J = \begin{bmatrix} \exp(a) & 0 \\ 0 & \exp(-d) \end{bmatrix}, \quad (2.7)$$

and we have the Jacobian matrix at $(\bar{H}, 0)$ as

$$J = \begin{bmatrix} a_1 & a_2 \\ 0 & a_3 \end{bmatrix}, \quad (2.8)$$

where $a_1 = \left(1 - b\bar{H} + \frac{\alpha\bar{H}}{(\beta + \bar{H})^2}\right)\exp\left(a - b\bar{H} - \frac{\alpha}{\beta + \bar{H}}\right)$, $a_2 = -\left(\frac{c\bar{H}}{e + \bar{H}}\right)\exp\left(a - b\bar{H} - \frac{\alpha}{\beta + \bar{H}}\right)$ and $a_3 = \exp\left(\frac{f\bar{H}}{e + \bar{H}} - d\right)$.

The Jacobian matrix of (2.3) evaluated at (H^*, P^*) is

$$J_{(H^*, P^*)}^* = \begin{bmatrix} 1 - bH^* + \frac{\alpha H^*}{(\beta + H^*)^2} + \frac{cH^* P^*}{(e + H^*)^2} & -\frac{cH^*}{e + H^*} \\ \frac{efP^*}{(e + H^*)^2} & 1 \end{bmatrix}. \quad (2.9)$$

The characteristic equation of J^* is given by

$$\lambda^2 - T\lambda + D = 0, \quad (2.10)$$

where

$$T = 2 - bH^* + \frac{\alpha H^*}{(\beta + H^*)^2} + \frac{cH^* P^*}{(e + H^*)^2},$$

$$D = 1 - bH^* + \frac{\alpha H^*}{(\beta + H^*)^2} + \frac{cH^* P^*}{(e + H^*)^2} + \frac{ecfH^* P^*}{(e + H^*)^3}.$$

From [38], let λ_1 and λ_2 be the eigenvalues of the Jacobian matrix (2.6) for some arbitrary equilibrium point (H, P) . We recall some topological classifications of the equilibrium points. The equilibrium point (H, P) is a sink (locally asymptotically stable) if $|\lambda_1| < 1$ and $|\lambda_2| < 1$. (H, P) is a source (locally unstable) if $|\lambda_1| > 1$ and $|\lambda_2| > 1$. (H, P) is a saddle if $|\lambda_1| > 1$ and $|\lambda_2| < 1$ (or $|\lambda_1| < 1$ and $|\lambda_2| > 1$). And, (H, P) is non-hyperbolic if either $|\lambda_1| = 1$ or $|\lambda_2| = 1$. As we know, the eigenvalue of the Jacobian matrix plays an important role in establishing the stability properties of the equilibrium points. Using the eigenvalues, we discuss the stability of the equilibrium points in the following lemmas:

Lemma 2. *The trivial equilibrium $(0, 0)$ is always a saddle and the predator-free equilibrium $(\bar{H}, 0)$ is a*

- (1) *sink if $|a_1| < 1$ and $|a_3| < 1$;*
- (2) *source if $|a_1| > 1$ and $|a_3| > 1$;*
- (3) *saddle if $|a_1| > 1$ and $|a_3| < 1$ (or $|a_1| < 1$ and $|a_3| > 1$).*

Lemma 3. *The coexisting equilibrium point*

- (1) *(H^*, P^*) is a sink if $D < 1$ and $|T| < D + 1$;*
- (2) *(H^*, P^*) is a source if $D > 1$ and $|T| < D + 1$ or $|T| > D + 1$;*
- (3) *(H^*, P^*) is a saddle if $0 < |T| + D + 1 < 2|T|$;*
- (4) *(H^*, P^*) is non-hyperbolic if $|T| = |D + 1|$, or $D = 1$ and $|T| \leq 2$.*

3. Bifurcations

Previously, we discussed the local stability properties of the equilibrium point (H^*, P^*) . Now, we study the bifurcation behavior, namely, flip and Neimark-Sacker bifurcations, of the model (2.3) at (H^*, P^*) by varying the parameter α and keeping all model parameters fixed. It should be noted that further analyses can hold for other parameters also. Also, stability properties of the existing period-two orbit and the invariant closed curve are discussed with the help of the CM theorem and normal form theory as in [38, 39]. The conditions for the model (2.3) to undergo both types of bifurcation are discussed below.

We know that the model can undergo a flip bifurcation if one of the eigenvalues of J^* is -1 and the other not 1 or -1 . Hence, we assume one eigenvalue as -1 , then, from (2.10),

$$4 - 2bH^* + \frac{2\alpha H^*}{(\beta + H^*)^2} + \frac{2cH^*P^*}{(e + H^*)^2} + \frac{ecfH^*P^*}{(e + H^*)^3} = 0, \quad (3.1)$$

$$\alpha = \frac{(H^* + \beta)^2}{2H^*} \left(-4 + 2bH^* - \frac{cefH^*P^*}{(e + H^*)^3} - \frac{2cH^*P^*}{(e + H^*)^2} \right) = \alpha_f,$$

where $\alpha = \alpha_f$ is the critical point of α that satisfies (3.1), and it is necessary for the flip bifurcation near the equilibrium point (H^*, P^*) for the model (2.3).

Let $\Omega_F = \{(a, b, c, d, e, f, \alpha, \beta) : \alpha = \alpha_f, a, b, c, d, e, f, \beta > 0\}$; at the critical parameter value $\alpha = \alpha_f$, the model exhibits flip bifurcation at (H^*, P^*) , when $\alpha = \alpha_f$ varies in the neighborhood of Ω_F .

Also, the model (2.3) admits the Neimark-Sacker bifurcation if the Jacobian matrix J^* has complex conjugate eigenvalues with a modulus value of one, and also satisfies the following conditions

$$(T(H^*, P^*))^2 - 4D(H^*, P^*) < 0 \text{ and } D(H^*, P^*) = 1, \quad (3.2)$$

which gives

$$\begin{aligned} A_1(\alpha) &= \left(2 - bH^* + \frac{\alpha H^*}{(\beta + H^*)^2} + \frac{cH^*P^*}{(e + H^*)^2} \right)^2 \\ &\quad - 4 \left(1 - bH^* + \frac{\alpha H^*}{(\beta + H^*)^2} + \frac{cH^*P^*}{(e + H^*)^2} + \frac{ecfH^*P^*}{(e + H^*)^3} \right) < 0, \\ A_2(\alpha) &= -bH^* + \frac{\alpha H^*}{(\beta + H^*)^2} + \frac{cH^*P^*}{(e + H^*)^2} + \frac{ecfH^*P^*}{(e + H^*)^3}. \end{aligned}$$

Now $A_2(\alpha) = 0$ gives

$$\alpha = \left(b - \frac{cefP^*}{(e + H^*)^3} - \frac{cP^*}{(e + H^*)^2} \right) (H^* + \beta)^2 = \alpha_h.$$

Let $\Omega_{NS} = \{(a, b, c, d, e, f, \alpha, \beta) : \alpha = \alpha_h, A_1(\alpha) < 0, a, b, c, d, e, f, \beta > 0\}$; at the critical parameter value $\alpha = \alpha_h$, the model (2.3) can exhibit Neimark-Sacker bifurcation near the equilibrium point (H^*, P^*) , when $\alpha = \alpha_h$ changes in the neighborhood of Ω_{NS} . Then, we conclude the above results in the following theorem:

Theorem 1. (i) If $\Omega_F = \{(a, b, c, d, e, f, \alpha, \beta) : \alpha = \alpha_f, a, b, c, d, e, f, \beta > 0\}$ exists and satisfies (3.1) at critical parameter value $\alpha = \alpha_f$, then the model (2.3) undergoes flip bifurcation.

(ii) If $\Omega_{NS} = \{(a, b, c, d, e, f, \alpha, \beta) : \alpha = \alpha_h, A_1(\alpha) < 0, a, b, c, d, e, f, \beta > 0\}$ exists and satisfies (3.2) at critical parameter value $\alpha = \alpha_h$, then the model (2.3) undergoes Neimark-Sacker bifurcation.

3.1. Flip bifurcation

Now we investigate the possible flip bifurcation of the model (2.3) at (H^*, P^*) . From the above discussion the model (2.3) undergoes flip bifurcation at $\alpha = \alpha_f$, where α varies in Ω_F . Given a perturbation $|\alpha_1| \ll 1$ of α_f , then perturbation of model (2.3) is described as

$$\begin{cases} H_{n+1} = H_n \exp \left[a - bH_n - \frac{\alpha_f + \alpha_1}{\beta + H_n} - \frac{cP_n}{e + H_n} \right], \\ P_{n+1} = P_n \exp \left[\frac{fH_n}{e + H_n} - d \right]. \end{cases} \quad (3.3)$$

Next by shifting (H^*, P^*) to the origin of (2.3) by using the transform $u_n = H_n - H^*$ and $z_n = P_n - P^*$, we have

$$\begin{cases} u_{n+1} = \gamma_1 u_n + \gamma_2 v_n + \gamma_3 \alpha_1 + \gamma_4 u_n^2 + \gamma_5 v_n^2 + \gamma_6 \alpha_1^2 \\ \quad + \gamma_7 u_n v_n + \gamma_8 u_n \alpha_1 + \gamma_9 v_n \alpha_1 + O((|u_n| + |v_n| + |\alpha_1|)^2), \\ v_{n+1} = \rho_1 u_n + \rho_2 v_n + \rho_3 \alpha_1 + \rho_4 u_n^2 + \rho_5 v_n^2 + \rho_6 \alpha_1^2 \\ \quad + \rho_7 u_n v_n + \rho_8 u_n \alpha_1 + \rho_9 v_n \alpha_1 + O((|u_n| + |v_n| + |\alpha_1|)^2), \end{cases} \quad (3.4)$$

where

$$\begin{aligned} \gamma_1 &= 1 - bH^* + \frac{cP^*H^*}{(e+H^*)^2} + \frac{\alpha_f H^*}{(\beta+H^*)^2}, \quad \gamma_2 = -\frac{cH^*}{e+H^*}, \quad \gamma_3 = -\frac{H^*}{\beta+H^*}, \\ \gamma_4 &= \frac{H^*}{2} \left(-b + \frac{cP^*}{(e+H^*)^2} + \frac{\alpha_f}{(\beta+H^*)^2} \right)^2 - b + \frac{ceP^*}{(e+H^*)^3} + \frac{\alpha_f \beta}{(\beta+H^*)^3}, \\ \gamma_5 &= \frac{c^2 H^*}{2(e+H^*)^2}, \quad \gamma_6 = \frac{H^*}{2(\beta+H^*)^2}, \quad \gamma_7 = -\frac{cH^*}{e+H^*} \left(-b + \frac{cP^*}{(e+H^*)^2} + \frac{\alpha_f}{(\beta+H^*)^2} \right) - \frac{ce}{(e+H^*)^2}, \\ \gamma_8 &= -\frac{H^*}{\beta+H^*} \left(-b + \frac{cP^*}{(e+H^*)^2} + \frac{\alpha_f}{(\beta+H^*)^2} \right) - \frac{\beta}{(\beta+H^*)^2}, \quad \gamma_9 = \frac{cH^*}{(e+H^*)(\beta+H^*)}, \\ \rho_1 &= \frac{feP^*}{(e+H^*)^2}, \quad \rho_2 = 1, \quad \rho_3 = 0, \quad \rho_4 = -\frac{feP^*}{(e+H^*)^3} + \frac{f^2 e^2 P^*}{2(e+H^*)^4}, \\ \rho_5 &= 0, \quad \rho_6 = 0, \quad \rho_7 = \frac{fe}{(e+H^*)^2}, \quad \rho_8 = 0, \quad \rho_9 = 0. \end{aligned}$$

Let us assume that the eigenvalues are $\lambda_1 = -1$ and $\lambda_2 = 3 - bH^* + \frac{cH^*P^*}{(e+H^*)^2} + \frac{\alpha_f H^*}{(\beta+H^*)^2}$ for the matrix J with $|\lambda_1| = 1$, $|\lambda_2| \neq 1$.

Next, we construct the non-singular matrix L as follows

$$L = \begin{pmatrix} \gamma_2 & \gamma_2 \\ -1 - \gamma_1 & \lambda_2 - \gamma_1 \end{pmatrix},$$

and we use the translation $\begin{pmatrix} u_n \\ v_n \end{pmatrix} = L \begin{pmatrix} U_n \\ V_n \end{pmatrix}$; then, (3.4) can be written as

$$\begin{cases} U_{n+1} = -U_n + F_1(u_n, v_n, \alpha_1) + O((|u_n| + |v_n| + |\alpha_1|)^2), \\ V_{n+1} = \lambda_2 V_n + (u_n, v_n, \alpha_1) + O((|u_n| + |v_n| + |\alpha_1|)^2), \end{cases} \quad (3.5)$$

where

$$\begin{aligned} F_1(u_n, v_n, \alpha_1) &= M_1 \alpha_1 + M_2 u_n^2 + M_3 v_n^2 + M_4 \alpha_1^2 + M_5 u_n v_n + M_6 u_n \alpha_1 + M_7 v_n \alpha_1, \\ F_2(u_n, v_n, \alpha_1) &= N_1 \alpha_1 + N_2 u_n^2 + N_3 v_n^2 + N_4 \alpha_1^2 + N_5 u_n v_n + N_6 u_n \alpha_1 + N_7 v_n \alpha_1, \end{aligned}$$

and

$$\begin{aligned} M_1 &= \frac{(\lambda_2 - \gamma_1)\gamma_3 - \gamma_2\rho_3}{\gamma_2(1 + \lambda_2)}, & M_2 &= \frac{(\lambda_2 - \gamma_1)\gamma_4 - \gamma_2\rho_4}{\gamma_2(1 + \lambda_2)}, & M_3 &= \frac{(\lambda_2 - \gamma_1)\gamma_5 - \gamma_2\rho_5}{\gamma_2(1 + \lambda_2)}, & M_4 &= \frac{(\lambda_2 - \gamma_1)\gamma_6 - \gamma_2\rho_6}{\gamma_2(1 + \lambda_2)}, \\ M_5 &= \frac{(\lambda_2 - \gamma_1)\gamma_7 - \gamma_2\rho_7}{\gamma_2(1 + \lambda_2)}, & M_6 &= \frac{(\lambda_2 - \gamma_1)\gamma_8 - \gamma_2\rho_8}{\gamma_2(1 + \lambda_2)}, & M_7 &= \frac{(\lambda_2 - \gamma_1)\gamma_9 - \gamma_2\rho_9}{\gamma_2(1 + \lambda_2)}, & N_1 &= \frac{(1 + \gamma_1)\gamma_3 + \gamma_2\rho_3}{\gamma_2(1 + \lambda_2)}, \\ N_2 &= \frac{(1 + \gamma_1)\gamma_4 + \gamma_2\rho_4}{\gamma_2(1 + \lambda_2)}, & N_3 &= \frac{(1 + \gamma_1)\gamma_5 + \gamma_2\rho_5}{\gamma_2(1 + \lambda_2)}, & N_4 &= \frac{(1 + \gamma_1)\gamma_6 + \gamma_2\rho_6}{\gamma_2(1 + \lambda_2)}, & N_5 &= \frac{(1 + \gamma_1)\gamma_7 + \gamma_2\rho_7}{\gamma_2(1 + \lambda_2)}, \\ N_6 &= \frac{(1 + \gamma_1)\gamma_8 + \gamma_2\rho_8}{\gamma_2(1 + \lambda_2)}, & N_7 &= \frac{(1 + \gamma_1)\gamma_9 + \gamma_2\rho_9}{\gamma_2(1 + \lambda_2)}. \end{aligned}$$

Now, let us assume G^c to be the CM; then, by using the CM theorem, we approximate the CM G^c of (3.5) at the origin for small changes in $\alpha_1 = 0$:

$$\begin{aligned} G^c(0, 0) &= \{(U_n, V_n) : V_n = h(U_n, \alpha_1)\} \\ &= \{(U_n, V_n) : V_n = c_1 \alpha_1 + c_2 U_n^2 + c_3 \alpha_1 U_n + c_4 \alpha_1^2 + O((|U_n| + \alpha_1)^2)\}. \end{aligned} \quad (3.6)$$

By substituting (3.5) on both sides of $V_n = h(U_n, \alpha_1)$, we have

$$\lambda_2 V_n + F_2(u_n, v_n, \alpha_1) = c_1 \alpha_1 + c_2 (-U_n + F_1(u_n, v_n, \alpha_1))^2 + c_3 \alpha_1 (-U_n + F_1(u_n, v_n, \alpha_1)) + c_4 \alpha_1^2 + O((|U_n| + \alpha_1)^2),$$

where

$$\begin{aligned} u_n &= \gamma_2 (U_n + V_n) = \gamma_2 (U_n + h(U_n, \alpha_1)), \\ v_n &= (-1 - \gamma_1) U_n + (\lambda_2 - \gamma_1) V_n = (-1 - \gamma_1) U_n + (\lambda_2 - \gamma_1) h(U_n, \alpha_1), \\ c_1 &= \frac{N_1}{1 - \lambda_2}, \quad c_2 = \frac{1}{1 - \lambda_2} \left[N_2 \gamma_2^2 + N_3 (1 + \gamma_1)^2 - N_5 \gamma_2 (1 + \gamma_1) \right], \\ c_3 &= \frac{1}{1 + \lambda_2} \left[-2c_2 M_1 - N_6 \gamma_2 + N_7 (1 + \gamma_1) - 2c_1 N_2 \gamma_2^2 \right. \\ &\quad \left. + 2c_1 N_3 (1 + \gamma_1) (\lambda_2 - \gamma_1) - c_1 N_5 \gamma_2 (\rho_2 - \gamma_1) \right], \\ c_4 &= \frac{1}{1 - \lambda_2} \left[c_1^2 N_2 \gamma_2^2 + c_1^2 N_3 (\lambda_2 - \gamma_1)^2 + c_1^2 N_5 \gamma_2 (\lambda_2 - \gamma_1) + c_1 N_6 \gamma_2 \right. \\ &\quad \left. + c_1 N_7 (\lambda_2 - \gamma_1) - c_2 M_1^2 + N_4 - M_1 c_3 \right]. \end{aligned}$$

Accordingly, on the CM G^c at the origin, we have

$$\begin{aligned} u_n^2 &= \gamma_2^2 (U_n^2 + 2U_n V_n + V_n^2), \\ u_n v_n &= -\gamma_2 (1 + \gamma_1) U_n^2 + \gamma_2 (\rho_2 - \gamma_1) U_n V_n + \gamma_2 (\lambda_2 - \gamma_1) V_n^2, \\ v_n^2 &= (1 + \gamma_1)^2 U_n^2 - 2(1 + \gamma_1) (\lambda_2 - \gamma_1) U_n V_n + (\lambda_2 - \gamma_1)^2 V_n^2, \end{aligned}$$

where

$$\begin{aligned} U_n V_n &= c_1 \alpha_1 U_n + c_2 U_n^3 + c_3 \alpha_1 U_n^2 + c_4 \alpha_1^2 U_n + O((|U_n| + |\alpha_1|)^3), \\ V_n^2 &= c_1^2 \alpha_1^2 + 2c_1 c_2 \alpha_1 U_n^2 + 2c_1 c_4 \alpha_1^3 + O((|U_n| + |\alpha_1|)^3). \end{aligned}$$

Moreover, the map confined to the CM $G^c(0, 0)$ takes the form

$$\begin{aligned} G^*(U_n) &= -U_n + F_1(u_n, v_n, \alpha_1) \\ &= -U_n + d_1 \alpha_1 + d_2 U_n^2 + d_3 U_n g^* + d_4 \alpha_1^2 + d_5 U_n^2 \alpha_1 \\ &\quad + d_6 U_n \alpha_1^2 + d_7 U_n^3 + d_8 \alpha_1^3 + O((|U_n| + |\alpha_1|)^3), \end{aligned}$$

where

$$\begin{aligned} d_1 &= M_1, \quad d_2 = M_2 \gamma_2^2 + M_3 (1 + \gamma_1)^2 - M_5 \gamma_2 (1 + \gamma_1), \\ d_3 &= 2c_1 M_2 \gamma_2^2 - 2c_1 M_3 (1 + \gamma_1) (\lambda_2 - \gamma_1) + c_1 M_5 \gamma_2 (\rho_2 - \gamma_1) + M_6 \gamma_2 - M_7 (1 + \gamma_1), \\ d_4 &= c_1^2 M_2 \gamma_2^2 + c_1^2 M_3 (\lambda_2 - \gamma_1)^2 + M_4 + c_1^2 M_5 \gamma_2 (\lambda_2 - \gamma_1) + c_1 M_6 \gamma_2 + c_1 M_7 (\lambda_2 - \gamma_1), \\ d_5 &= 2c_3 M_2 \gamma_2^2 + 2c_1 c_2 M_2 \gamma_2^2 - 2c_3 M_3 (1 + \gamma_1) (\lambda_2 - \gamma_1) + 2c_1 c_2 M_3 (\lambda_2 - \gamma_1)^2 \\ &\quad + c_3 M_5 \gamma_2 (\rho_2 - \gamma_1) + 2c_1 c_2 M_5 \gamma_2 (\lambda_2 - \gamma_1) + c_2 M_6 \gamma_2 + c_2 M_7 (\lambda_2 - \gamma_1), \\ d_6 &= 2c_4 M_2 \gamma_2^2 + 2c_1 c_3 M_2 \gamma_2^2 - 2c_4 M_3 (1 + \gamma_1) (\lambda_2 - \gamma_1) + 2c_1 c_3 M_3 (\lambda_2 - \gamma_1)^2 \\ &\quad + c_4 M_5 \gamma_2 (\rho_2 - \gamma_1) + 2c_1 c_3 M_5 \gamma_2 (\lambda_2 - \gamma_1) + c_3 M_6 \gamma_2 + c_3 M_7 (\lambda_2 - \gamma_1), \\ d_7 &= 2c_2 M_2 \gamma_2^2 - 2c_2 M_3 (1 + \gamma_1) (\lambda_2 - \gamma_1) + c_2 M_5 \gamma_2 (\rho_2 - \gamma_1), \\ d_8 &= 2c_1 c_4 M_2 \gamma_2^2 + 2c_1 c_4 M_3 (\lambda_2 - \gamma_1)^2 + 2c_1 c_4 M_5 \gamma_2 (\lambda_2 - \gamma_1) + c_4 M_6 \gamma_2 + c_4 M_7 (\lambda_2 - \gamma_1). \end{aligned}$$

Finally, from [40], we define Δ_1 and Δ_2 as follows:

$$\Delta_1 = \left(G_{U_n \alpha_1}^* + \frac{1}{2} G_{\alpha_1}^* G_{U_n U_n}^* \right) \Big|_{(U_n, \alpha_1) = (0,0)} = d_3 + d_1 d_2, \quad (3.7)$$

$$\Delta_2 = \left(\frac{1}{6} G_{U_n U_n U_n}^* + \left(\frac{1}{2} G_{U_n U_n}^* \right)^2 \right) \Big|_{(U_n, \alpha_1) = (0,0)} = d_7 + d_2^2. \quad (3.8)$$

Therefore, we have the following findings about flip bifurcation from the aforementioned study.

Theorem 2. *If $\Delta_1 \neq 0$ and $\Delta_2 \neq 0$, the model (2.3) exhibits a flip bifurcation at (H^*, P^*) while changing the parameter Δ nearby Δ_1 . Moreover, if $\Delta_2 > 0$ (or $\Delta_2 < 0$) then the existing period two orbits from (H^*, P^*) are stable (or unstable).*

3.2. Neimark-Sacker bifurcation

Now we analyze the properties of possible Neimark-Sacker bifurcation around (H^*, P^*) for model (2.3) if, for instance, (3.2) holds for some α_n . Given a perturbation $|\alpha_2| \ll 1$ of α_n , perturbation of model (2.3) is described as

$$\begin{cases} H_{n+1} = H_n \exp \left[a - bH_n - \frac{\alpha_n + \alpha_2}{\beta + H_n} - \frac{cP_n}{e + H_n} \right] \\ P_{n+1} = P_n \exp \left[\frac{fH_n}{e + H_n} - d \right]. \end{cases} \quad (3.9)$$

Let us use the transforms $u_n = H_n - H^*$ and $v_n = P_n - P^*$ and shift (H^*, P^*) to $(0, 0)$; the model (3.9) takes the form

$$\begin{cases} u_{n+1} = (u_n + H^*) \exp \left[a - bH_n - \frac{\alpha_n + \alpha_2}{\beta + H_n} - \frac{cP_n}{e + H_n} \right] - H^*, \\ v_{n+1} = (v_n + P^*) \exp \left[\frac{fH_n}{e + H_n} - d \right] - P^*. \end{cases} \quad (3.10)$$

Then, the Taylor expansion of (3.10) at the origin, up to order three, is

$$\begin{cases} u_{n+1} = \delta_1 u_n + \delta_2 v_n + \delta_3 u_n^2 + \delta_4 u_n v_n + \delta_5 v_n^2 + \delta_6 u_n^3 \\ \quad + \delta_7 u_n^2 v_n + \delta_8 u_n v_n^2 + \delta_9 v_n^3 + O((|u_n| + |v_n|)^3), \\ v_{n+1} = \rho_1 u_n + \rho_2 v_n + \rho_3 u_n^2 + \rho_4 u_n v_n + \rho_5 v_n^2 + \rho_6 u_n^3 \\ \quad + \rho_7 u_n^2 v_n + \rho_8 u_n v_n^2 + \rho_9 v_n^3 + O((|u_n| + |v_n|)^3), \end{cases} \quad (3.11)$$

where

$$\begin{aligned}
 \delta_1 &= 1 - bH^* + \frac{cP^*H^*}{(e+H^*)^2} + \frac{\alpha_h H^*}{(\beta+H^*)^2}, \delta_2 = -\frac{cH^*}{e+H^*}, \\
 \delta_3 &= \frac{H^*}{2} \left(-b + \frac{cP^*}{(e+H^*)^2} + \frac{\alpha_h}{(\beta+H^*)^2} \right)^2 - b + \frac{ceP^*}{(e+H^*)^3} + \frac{\alpha_h \beta}{(\beta+H^*)^3}, \\
 \delta_4 &= -\frac{cH^*}{e+H^*} \left(-b + \frac{cP^*}{(e+H^*)^2} + \frac{\alpha_h}{(\beta+H^*)^2} \right) - \frac{ce}{(e+H^*)^2}, \delta_5 = \frac{c^2 H^*}{2(e+H^*)^2}, \\
 \delta_6 &= \frac{H^*}{6} \left(-b + \frac{cP^*}{(e+H^*)^2} + \frac{\alpha_h}{(\beta+H^*)^2} \right)^3 + \frac{1}{2} \left(-b + \frac{cP^*}{(e+H^*)^2} + \frac{\alpha_h}{(\beta+H^*)^2} \right)^2 \\
 &\quad - \left(\frac{cH^*P^*}{(e+H^*)^3} + \frac{\alpha_h H^*}{(\beta+H^*)^3} \right) \left(-b + \frac{cP^*}{(e+H^*)^2} + \frac{\alpha_h}{(\beta+H^*)^2} \right) - \frac{ceP^*}{(e+H^*)^4} - \frac{\alpha_h \beta}{(\beta+H^*)^4}, \\
 \delta_7 &= -\frac{cH^*}{2(e+H^*)} \left(-b + \frac{cP^*}{(e+H^*)^2} + \frac{\alpha_h}{(\beta+H^*)^2} \right)^2 - \frac{ce}{(e+H^*)^2} \left(-b + \frac{cP^*}{(e+H^*)^2} + \frac{\alpha_h}{(\beta+H^*)^2} \right) \\
 &\quad + \frac{cH^*}{e+H^*} \left(\frac{cP^*}{(e+H^*)^3} + \frac{\alpha_h}{(\beta+H^*)^3} \right) + \frac{ce}{(e+H^*)^3}, \\
 \delta_8 &= \frac{c^2 H^*}{2(e+H^*)^2} \left(-b + \frac{cP^*}{(e+H^*)^2} + \frac{\alpha_h}{(\beta+H^*)^2} \right) + \frac{c^2 e - c^2 H^*}{2(e+H^*)^3}, \delta_9 = -\frac{c^3 H^*}{6(e+H^*)^3}, \\
 \rho_1 &= \frac{feP^*}{(e+H^*)^2}, \rho_2 = 1, \rho_3 = -\frac{feP^*}{(e+H^*)^3} + \frac{f^2 e^2 P^*}{2(e+H^*)^4}, \\
 \rho_4 &= \frac{fe}{(e+H^*)^2}, \rho_5 = 0, \rho_6 = \frac{fe}{(e+H^*)^4} - \frac{f^2 e^2 P^*}{(e+H^*)^5} + \frac{f^3 e^3 P^*}{6(e+H^*)^6}, \\
 \rho_7 &= -\frac{fe}{(e+H^*)^3} + \frac{f^2 e^2}{2(e+H^*)^4}, \rho_8 = 0, \rho_9 = 0.
 \end{aligned}$$

The characteristic polynomial equation associated with the linearized system of (3.10) at the origin:

$$\lambda^2 + q_1(\alpha_2)\lambda + q_2(\alpha_2) = 0, \quad (3.12)$$

where

$$\begin{aligned}
 q_1(\alpha_2) &= \left(-1 + bH^* - \frac{(\alpha_f + \alpha_2)H^*}{(\beta + H^*)^2} - \frac{cH^*P^*}{(e + H^*)^2} \right) A_1 - A_2, \\
 q_2(\alpha_2) &= \left(1 - bH^* + \frac{(\alpha_f + \alpha_2)H^*}{(\beta + H^*)^2} + \frac{cH^*P^*}{(e + H^*)^2} + \frac{ecfH^*P^*}{(e + H^*)^3} \right) A_1 A_2,
 \end{aligned}$$

with $A_1 = \exp\left(a - bH^* - \frac{(\alpha_f + \alpha_2)}{\beta + H^*} - \frac{cP^*}{e + H^*}\right)$ and $A_2 = \exp\left(\frac{fH^*}{e + H^*} - d\right)$. Now, the roots of (3.12) are expressed as a pair of complex conjugates:

$$\lambda_{1,2} = \frac{1}{2} \left[-q_1(\alpha_2) \pm i \sqrt{4q_2(\alpha_2) - (q_1(\alpha_2))^2} \right].$$

Since $(a, b, c, d, e, f, \alpha, \beta) \in \Omega_{NS}$, we have that $|\lambda_{1,2}| = \sqrt{q_2(\alpha_2)}$ and

$$\begin{aligned}
 \left. \frac{d|\lambda_{1,2}|}{d\alpha_2} \right|_{\alpha_2=0} &= \frac{1}{2\sqrt{q_2(0)}} \left\{ \frac{H^*}{(\beta + H^*)^2} - \frac{1}{\beta + H^*} \right. \\
 &\quad \left. \times \left(1 - bH^* + \frac{\alpha_h H^*}{(\beta + H^*)^2} + \frac{cH^*P^*}{(e + H^*)^2} + \frac{ecfH^*P^*}{(e + H^*)^3} \right) \right\} < 0. \quad (3.13)
 \end{aligned}$$

Further, we assume that $q_1(0) = -2 + bH^* - \frac{\alpha_h H^*}{(\beta + H^*)^2} - \frac{cH^*P^*}{(e + H^*)^2} \neq 0, -1$ and (2.6) implies that $q_1(0) \neq \pm 2, 0, -1$, which means that $\lambda_1^k, \lambda_2^k \neq 1$ for $k = 1, 2, 3, 4$ when $\alpha_2 = 0$. We only require that $q_1(0) \neq 0, 1$, which we can attain if it satisfies

$$bH^* - \frac{\alpha_h H^*}{(\beta + H^*)^2} - \frac{cH^*P^*}{(e + H^*)^2} \neq 2, 3. \quad (3.14)$$

Letting $\alpha_2 = 0$, $\xi = -\frac{q_1(0)}{2}$ and $\theta = \frac{\sqrt{4q_2(0)-q_1^2(0)}}{2}$, we construct the non-singular matrix

$$L = \begin{pmatrix} \delta_2 & 0 \\ \xi - \delta_1 & \theta \end{pmatrix},$$

and we use the translation $\begin{pmatrix} u_n \\ v_n \end{pmatrix} = L \begin{pmatrix} U_n \\ V_n \end{pmatrix}$; thus, the model (3.9) takes the form

$$\begin{cases} U_{n+1} = \xi U_n + \theta V_n + Q(U_n, V_n) + O((|U_n| + |V_n|)^3), \\ V_{n+1} = -\theta U_n + \xi V_n + R(U_n, V_n) + O((|U_n| + |V_n|)^3), \end{cases} \quad (3.15)$$

where

$$\begin{aligned} Q(U_n, V_n) = & \frac{1}{\delta_2} [\{ \delta_3 \delta_2^2 + \delta_4 \delta_2 (\xi - \delta_1) + \delta_5 (\xi - \delta_1)^2 \} U_n^2 + \{ \delta_4 \delta_2 \theta + 2\theta \delta_5 (\xi - \delta_1) \} U_n V_n \\ & + \delta_5 \theta^2 V_n^2 + \{ \delta_6 \delta_2^3 + \delta_7 \delta_2^2 (\xi - \delta_1) + \delta_8 \delta_2 (\xi - \delta_1)^2 + \delta_9 (\xi - \delta_1)^3 \} U_n^3 \\ & + \{ \delta_7 \delta_2^2 + 2\theta \delta_8 \delta_2 (\xi - \delta_1) + 3\theta \delta_9 (\xi - \delta_1)^2 \} U_n^2 V_n \\ & + \{ \theta^2 \delta_8 \delta_2 + 3\theta^2 \delta_9 (\xi - \delta_1) \} U_n V_n^2 + \theta^3 \delta_9 V_n^3], \end{aligned}$$

$$\begin{aligned} R(U_n, V_n) = & \frac{1}{\delta_2 \theta} [\{ \delta_2^2 (\delta_3 (\delta_1 - \xi) + \delta_2 \rho_3) + \delta_2 (\xi - \delta_1) (\delta_4 (\delta_1 - \xi) + \delta_2 \rho_4) \\ & + (\xi - \delta_1)^2 (\delta_5 (\delta_1 - \xi) + \delta_2 \rho_5) \} U_n^2 + \{ \theta \delta_2 (\delta_4 (\delta_1 - \xi) + \delta_2 \rho_4) \\ & + 2\theta (\xi - \delta_1) (\delta_5 (\delta_1 - \xi) + \delta_2 \rho_5) \} U_n V_n + \theta^2 \{ \delta_5 (\delta_1 - \xi) + \delta_2 \rho_5 \} V_n^2 \\ & + \{ \delta_2^3 (\delta_6 (\delta_1 - \xi) + \delta_2 \rho_6) + \delta_2^2 (\xi - \delta_1) (\delta_7 (\delta_1 - \xi) + \delta_2 \rho_7) \\ & + \delta_2 (\xi - \delta_1)^2 (\delta_8 (\delta_1 - \xi) + \delta_2 \rho_8) - (\xi - \delta_1)^3 (\delta_9 (\delta_1 - \xi) + \delta_2 \rho_9) \} U_n^3 \\ & + \{ \theta \delta_2^2 (\delta_7 (\delta_1 - \xi) + \delta_2 \rho_7) + 2\theta \delta_2 (\xi - \delta_1) (\delta_8 (\delta_1 - \xi) + \delta_2 \rho_8) \\ & + 3\theta (\xi - \delta_1)^2 (\delta_9 (\delta_1 - \xi) + \delta_2 \rho_9) \} U_n^2 V_n + \{ \theta^2 \delta_2 (\delta_8 (\delta_1 - \xi) + \delta_2 \rho_8) \\ & + 3\theta^2 (\xi - \delta_1) (\delta_9 (\delta_1 - \xi) + \delta_2 \rho_9) \} U_n V_n^2 + \theta^3 (\delta_9 (\delta_1 - \xi) + \delta_2 \rho_9) V_n^3]. \end{aligned}$$

Next, we require the non zero quantity a^* to ensure that (3.9) admits Neimark-Sacker NS bifurcation.

$$a^* = -Re \left[\frac{(1-2\lambda)\bar{\lambda}^2}{1-\lambda} \xi_{11} \xi_{20} \right] - \frac{1}{2} |\xi_{11}|^2 - |\xi_{02}|^2 + Re(\bar{\lambda} \xi_{21}), \quad (3.16)$$

where

$$\begin{aligned} \xi_{20} &= \frac{1}{8} [(Q_{U_n U_n} - Q_{V_n V_n} + 2R_{U_n V_n}) + i(R_{U_n U_n} - R_{V_n V_n} - 2Q_{U_n V_n})], \\ \xi_{11} &= \frac{1}{4} [(Q_{U_n U_n} + Q_{V_n V_n}) + i(R_{U_n U_n} + R_{V_n V_n})], \\ \xi_{02} &= \frac{1}{8} [(Q_{U_n U_n} - Q_{V_n V_n} - 2R_{U_n V_n}) + i(R_{U_n U_n} - R_{V_n V_n} + 2Q_{U_n V_n})], \\ \xi_{21} &= \frac{1}{16} [(Q_{U_n U_n U_n} + Q_{U_n V_n V_n} + R_{U_n U_n V_n} + R_{V_n V_n V_n}) \\ & \quad + i(R_{U_n U_n U_n} + R_{U_n V_n V_n} - Q_{U_n U_n V_n} - Q_{V_n V_n V_n})]. \end{aligned}$$

Finally, from [38], we can state the following findings:

Theorem 3. *If (3.13) and (3.14) hold and the quantity a^* is non zero then the model (3.1) admits Neimark-Sacker bifurcation at (H^*, P^*) when α_n changes in the neighborhood of Ω_{NS} . Additionally, the quantity $a^* < 0$ (or resp. $a^* > 0$); then, the stable (or resp. unstable) invariant closed curve from (H^*, P^*) starts to bifurcate.*

4. Chaos control

The theory of chaos control and bifurcation is known to be an essential area of current research. In particular, it has significant uses in biological and engineering sciences. Its features have emerged in ecological models. The nature of discrete-time population models is mostly unstable and chaotic in contrast to the continuous-time models. It is known that the logistic difference equation (logistic map) and the Ricker model [37] are the discrete analogs of the logistic differential equation [9]. The logistic map is derived from the logistic differential equation by using Euler approximation, taking the finite difference quotient as $\Delta t = 1$, i.e., the time step is one generation. The sequence of periodic orbits starts oscillate from stable point like period 2, period 4, period 8, ..., cycles and finally enter into the chaotic regime for many difference equations; this collection of such simple difference equations have been reported in ecology [41]. The Neimark-Sacker bifurcation is similar to the Hopf bifurcation in the continuous system. Similarly, there has been a lot of research work on the presence of complex and chaotic nature in the two-dimensional discrete prey-predator system, this chaotic dynamics absent in the continuous time system [42]. Further, it is important to introduce the appropriate methods for controlling chaos to prevent unexpected scenarios.

First, we use the state feedback control method as in [43, 44] to control the chaotic system. For the model (2.3) we consider the following corresponding controlled model:

$$\begin{cases} H_{n+1} = H_n \exp\left(a - bH_n - \frac{\alpha}{\beta + H_n} - \frac{cP_n}{e + H_n}\right) - u(H_n, P_n) = f(H_n, P_n), \\ P_{n+1} = P_n \exp\left(\frac{fH_n}{e + H_n} - d\right) = g(H_n, P_n), \end{cases} \quad (4.1)$$

where $u(H_n, P_n) = h_1(H_n - H^*) + h_2(P_n - P^*)$ is the feedback controlling force with feedback gains h_1 and h_2 , and (H^*, P^*) is the unique positive interior equilibrium point of (4.1). Consider the controlled model (4.1) whose Jacobian matrix at (H^*, P^*) is given as

$$J(H^*, P^*) = \begin{pmatrix} b_{11} - h_1 & b_{12} - h_2 \\ b_{21} & b_{22} \end{pmatrix}, \quad (4.2)$$

where

$$b_{11} = 1 - bH^* + \frac{\alpha H^*}{(\beta + H^*)^2} + \frac{cH^*P^*}{(e + H^*)^2}, b_{12} = -\frac{cH^*}{e + H^*}, b_{21} = \frac{efP^*}{(e + H^*)^2}, b_{22} = 1.$$

Then we have the characteristic polynomial of $J(H^*, P^*)$ as

$$\lambda^2 - (b_{11} + b_{22} - h_1)\lambda + b_{22}(b_{11} - h_1) - b_{21}(b_{12} - h_2) = 0. \quad (4.3)$$

Let λ_1 and λ_2 be the eigenvalues of (4.3); then, we obtain

$$\lambda_1 + \lambda_2 = b_{11} + b_{22} - h_1, \lambda_1\lambda_2 = b_{22}(b_{11} - h_1) - b_{21}(b_{12} - h_2). \quad (4.4)$$

Then, the lines of marginal stability are derived by solving $\lambda_1 = \pm 1$ and $\lambda_1\lambda_2 = 1$, assuming that $|\lambda_{1,2}| \ll 1$. If $\lambda_1\lambda_2 = 1$, using the second part of (4.4), we have

$$L_1 : b_{11}b_{22} - b_{21}b_{12} - 1 = h_1b_{22} - h_2b_{21}. \quad (4.5)$$

Next, if $\lambda_1 = 1$, and using (4.4), we get

$$L_2 : h_1(1 - b_{22}) + h_2b_{21} = b_{11} + b_{22} - 1 - b_{11}b_{22} + b_{21}b_{12}. \quad (4.6)$$

Also, if $\lambda_1 = -1$, and using (4.4), we obtain

$$L_3 : h_1(1 + b_{22}) - h_2b_{21} = b_{11} + b_{22} + 1 + b_{11}b_{22} - b_{21}b_{12}. \quad (4.7)$$

Then the triangular region enclosed by lines L_1, L_2, L_3 have stable eigenvalues.

Next, we study a chaos controlling technique based on the OGY control method as in [26]. By taking α as the control parameter, we rewrite the model (2.3) as follows:

$$\begin{cases} H_{n+1} = H_n \exp\left(a - bH_n - \frac{\alpha}{\beta+H_n} - \frac{cP_n}{e+H_n}\right) = f_1(H_n, P_n), \\ P_{n+1} = P_n \exp\left(\frac{fH_n}{e+H_n} - d\right) = f_2(H_n, P_n). \end{cases} \quad (4.8)$$

Further, α must lie in some interval $|\alpha - \alpha_0| < \delta$ with $\delta > 0$, and α_0 denotes the nominal value, for which the model (2.3) has chaotic dynamics. Now, we apply the state feedback control strategy to shift the trajectory to the desired state. Let (H^*, P^*) be the unstable equilibrium point of the model (2.3) in the chaotic state due to Neimark-Sacker bifurcation; then, model (2.3) can be approximated near (H^*, P^*) by the following linear map:

$$\begin{bmatrix} H_{n+1} - H^* \\ P_{n+1} - P^* \end{bmatrix} \approx A \begin{bmatrix} H_n - H^* \\ P_n - P^* \end{bmatrix} + B[\alpha - \alpha_0], \quad (4.9)$$

where

$$A = \begin{bmatrix} \frac{\partial f_1(H^*, P^*, \alpha_0)}{\partial H_n} & \frac{\partial f_1(H^*, P^*, \alpha_0)}{\partial P_n} \\ \frac{\partial f_2(H^*, P^*, \alpha_0)}{\partial H_n} & \frac{\partial f_2(H^*, P^*, \alpha_0)}{\partial P_n} \end{bmatrix}, B = \begin{bmatrix} \frac{\partial f_1(H^*, P^*, \alpha_0)}{\partial \alpha} \\ \frac{\partial f_2(H^*, P^*, \alpha_0)}{\partial \alpha} \end{bmatrix} = \begin{bmatrix} -\frac{H^*}{\beta+H^*} \\ 0 \end{bmatrix}.$$

It is easy to see that model (4.8) is controllable provided that the following matrix

$$C = [B : AB] = \begin{bmatrix} -\frac{H^*}{\beta+H^*} & \left(\frac{\partial f_1(H^*, P^*, \alpha_0)}{\partial H_n}\right) \frac{-H^*}{\beta+H^*} \\ 0 & \left(\frac{\partial f_2(H^*, P^*, \alpha_0)}{\partial H_n}\right) \frac{-H^*}{\beta+H^*} \end{bmatrix} \quad (4.10)$$

has rank 2. Furthermore, assume that $\frac{-H^*}{\beta+H^*} \neq 0$ and $\frac{\partial f_2(H^*, P^*, \alpha_0)}{\partial H_n} \neq 0$; then, model (4.8) is controllable.

Next, we assume that $[\alpha - \alpha_0] = -K \begin{bmatrix} H_n - H^* \\ P_n - P^* \end{bmatrix}$, where $K = \begin{bmatrix} s_1 & s_2 \end{bmatrix}$; then, model (4.8) can be written as

$$\begin{bmatrix} H_{n+1} - H^* \\ P_{n+1} - P^* \end{bmatrix} \approx [A - BK] \begin{bmatrix} H_n - H^* \\ P_n - P^* \end{bmatrix}. \quad (4.11)$$

Then, the controller model is given by

$$\begin{cases} H_{n+1} = H_n \exp\left(a - bH_n - \frac{\alpha_0 - s_1(H_n - H^*) - s_2(P_n - P^*)}{\beta + H_n} - \frac{cP_n}{e + H_n}\right), \\ P_{n+1} = P_n \exp\left(\frac{fH_n}{e + H_n} - d\right). \end{cases} \quad (4.12)$$

Moreover, equilibrium point (H^*, P^*) is locally asymptotically stable if and only if both eigenvalues of the matrix $A - BK$, say, λ_1 and λ_2 , lie in an open unit disk. Then, the matrix $A - BK$ can be written as

$$A - BK = \begin{bmatrix} b_{11} - \theta s_1 & b_{12} - \theta s_1 \\ b_{21} & b_{22} \end{bmatrix}, \quad (4.13)$$

where

$$b_{11} = 1 - bH^* + \frac{\alpha_0 H^*}{(\beta + H^*)^2} + \frac{cH^* P^*}{(e + H^*)^2}, \quad b_{12} = -\frac{cH^*}{e + H^*}, \quad b_{21} = \frac{efP^*}{(e + H^*)^2}, \\ b_{22} = 1, \quad \theta = -\frac{H^*}{\beta + H^*}.$$

Then, the characteristic polynomial of (4.13) is given by

$$\lambda^2 - (b_{11} + b_{22} - \theta s_1)\lambda + b_{22}(b_{11} - \theta s_1) + b_{21}(\theta s_2 - b_{12}) = 0. \quad (4.14)$$

Then, the lines of marginal stability can be obtained, that is,

$$L_1 : b_{22}(b_{11} - \theta s_1) + b_{21}(\theta s_2 - b_{12}) = 1, \quad (4.15)$$

$$L_2 : b_{11} + b_{22} = 1 + \theta s_1 + b_{22}(b_{11} - \theta s_1) + b_{21}(\theta s_2 - b_{12}), \quad (4.16)$$

$$L_3 : \theta s_1 = b_{11} + b_{22} + 1 + b_{22}(b_{11} - \theta s_1) + b_{21}(\theta s_2 - b_{12}). \quad (4.17)$$

Then, stable eigenvalues lie within the triangular region in the s_1, s_2 -plane bounded by the straight lines L_1, L_2, L_3 for the model's parametric values.

Next, we apply a hybrid control feedback methodology [21, 25, 45] for the control of flip and Neimark-Sacker bifurcations of the model near the equilibrium point (H^*, P^*) ; then, the controlled model can be written as

$$\begin{cases} H_{n+1} = \epsilon H_n \exp\left(a - bH_n - \frac{\alpha}{\beta + H_n} - \frac{cP_n}{e + H_n}\right) + (1 - \epsilon)H_n, \\ P_{n+1} = \epsilon P_n \exp\left(\frac{fH_n}{e + H_n} - d\right) + (1 - \epsilon)P_n, \end{cases} \quad (4.18)$$

where $0 < \epsilon < 1$ is the controlled strategy of a combination of both feedback control and parameter perturbation. The Jacobian matrix evaluated for the model (4.18) at (H^*, P^*) is given by

$$\begin{bmatrix} \epsilon \left(1 - bH^* + \frac{\alpha H^*}{(\beta + H^*)^2} + \frac{cH^* P^*}{(e + H^*)^2}\right) + 1 - \epsilon & -\frac{\epsilon c H^*}{e + H^*} \\ \frac{\epsilon e f P^*}{(e + H^*)^2} & 1 \end{bmatrix}. \quad (4.19)$$

Note, one can select appropriate values for ϵ to ensure that all eigenvalues of the above matrix satisfy $|\lambda_{1,2}| < 1$.

5. Numerical simulations

In this section, we provide a numerical simulation to ensure our theoretical analysis. The numerical iteration used to validate our results is similar to the processes described in [27, 28, 36, 44, 46]. The mathematical software Matlab (2018a) has been used to plot the numerical graphs. The computational approach provides fascinating details about how ecological systems function. Analytical approaches are exact and wide, but they only operate with the most fundamental models. The parameter values used here are only for illustrative purposes; neither experiments nor field research was used to obtain them [29–31]. Here, all parameters are considered positive values for which the model (2.3) has at least one positive interior equilibrium point (coexistence of both populations). Also, the chosen parameter values for the considered model (2.3) are biologically feasible.

Next, the conditions for the occurrence of two possible bifurcation behaviors of the model (2.3) were examined by varying the Allee parameter, namely, flip and Neimark-Sacker bifurcation verified numerically. It is also shown with the help of bifurcation diagrams. For this, we take two sets of parameter values assuming $\alpha < a\beta$, and described them in the following cases:

Case (i): Show the model (2.3) exhibits flip bifurcation with the fixed parametric values of $a = 5.5$, $b = 5.5$, $c = 20$, $d = 0.1$, $e = 10$, $f = 2$, $\beta = 0.5$, while varying $\alpha = (0, 2]$. We obtained the unique interior positive equilibrium points (H^*, P^*) for the various values of α given in Table 1. At the critical point $\alpha = \alpha_f = 1.5833188$, the model (2.3) has the unique equilibrium point $(H^*, P^*) = (0.526316, 0.559233)$, and (2.10) becomes

$$\lambda^2 + 0.0504708\lambda - 0.949529 = 0,$$

which shows that, $\lambda_1, \lambda_2 = 0.949529, -1$ are the eigenvalues of (2.9), Then, it satisfies the condition. It ensures the occurrence of flip bifurcation near the interior equilibrium point for the model (2.3). Also, for $\alpha = 0.20$, the model (2.3) shows chaotic behavior, and by further increasing, it shows period-16 at $\alpha = 0.37$, period-8 at $\alpha = 0.43$, period-4 at $\alpha = 0.50$, period-2 at $\alpha = 1.25$, and stable equilibrium point at $\alpha = 1.70$. The different states of the model (2.3) are plotted for different values of α in the time plot and phase portrait in Figures 1 and 2, respectively. It indicates that the model becomes stable from chaos by the reverse period-doubling phenomenon. So, the existence of flip bifurcation for the model (2.3) is shown in Figure 3(a). Also, the existence of chaos is confirmed by plotting the corresponding largest Lyapunov exponent in Figure 3(b). Further, from (3.7) and (3.8), we obtain $\Delta_1 = 0.415148 \neq 0$, $\Delta_2 = -2.22965 \neq 0$ and the property of the existing flip bifurcation which is illustrated in Theorem 2.

Table 1. The equilibrium point values for Case (i).

α	H^*	P^*
0.20	0.526316	1.268630
0.37	0.526316	1.181450
0.43	0.526316	1.150680
0.50	0.526316	1.114780
1.25	0.526316	0.730165
1.70	0.526316	0.499396

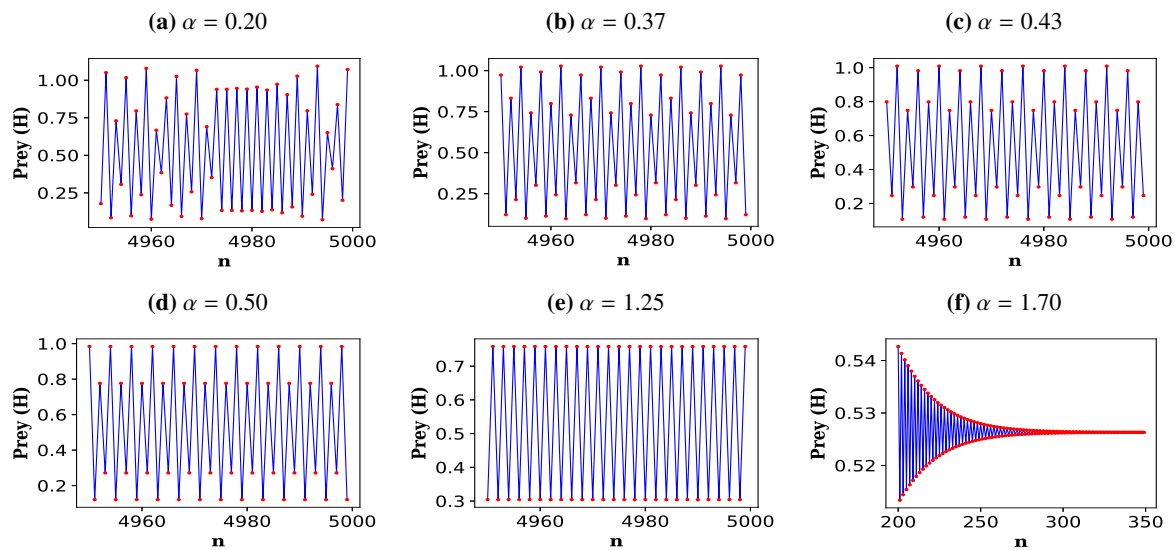


Figure 1. Time-series plots of H_n vs n for the occurrence of flip bifurcation, where (a) is a chaotic orbit, (b) is period-16, (c) is period-8, (d) is period-4, (e) is period-2 and, in (f) it eventually reaches the non-zero equilibrium point.

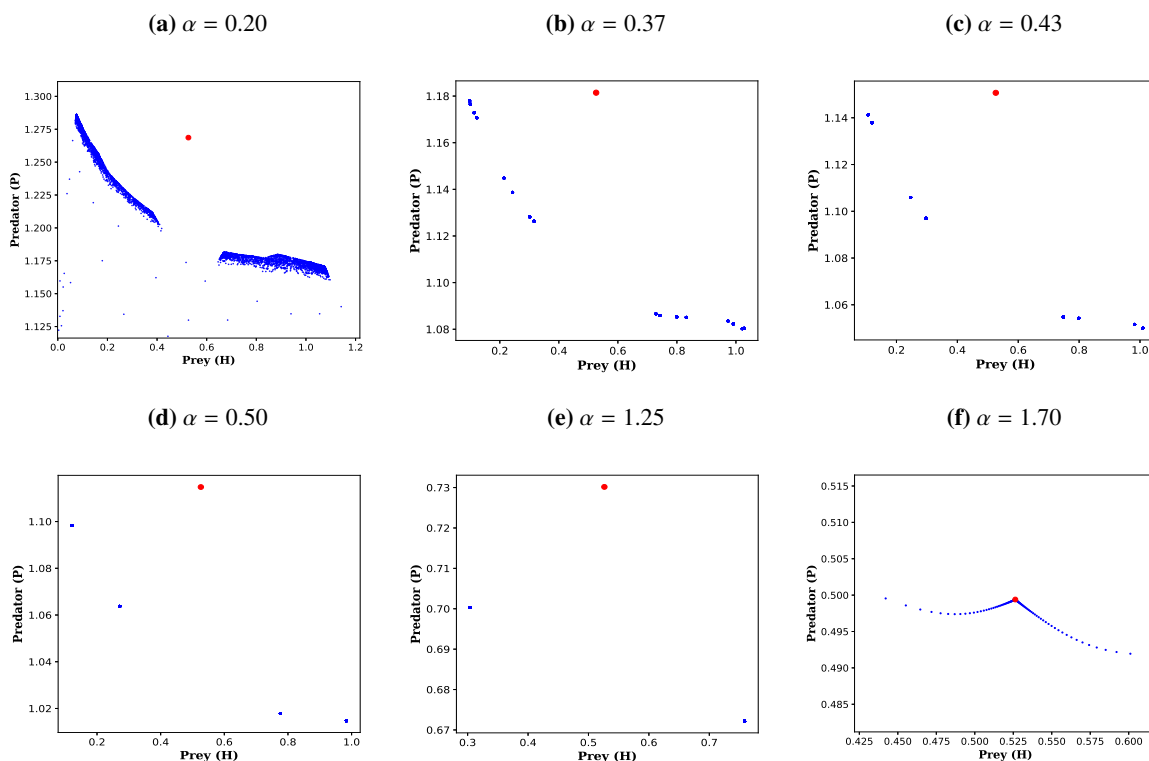


Figure 2. Phase portraits for the occurrence of flip bifurcation where (a) is a chaotic orbit, (b) is period-16, (c) is period-8, (d) is period-4, (e) is period-2 and, in (f) it eventually reaches the non-zero equilibrium point. The asterisk symbol represents the unique interior equilibrium point and its values are given in Table 1.

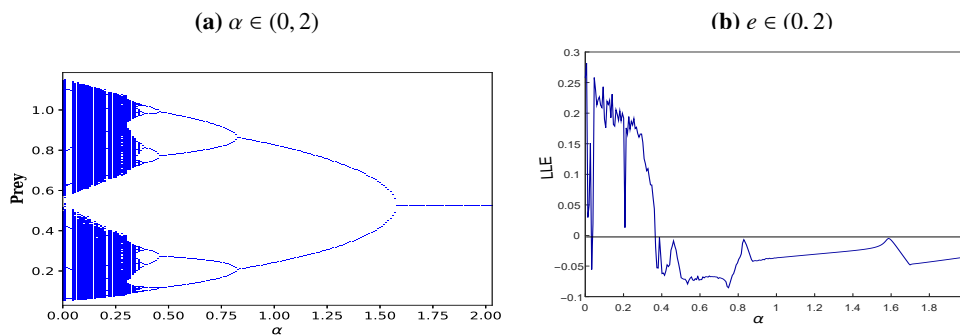


Figure 3. (a) Flip bifurcation diagram of the model (2.3) in the (α, H) plane and its largest Lyapunov exponent in (b), correspondingly, with $a = 5.5$, $b = 5.5$, $c = 20$, $d = 0.1$, $e = 10$, $f = 2$, $\beta = 0.5$ and varying $\alpha = (0, 2]$.

Case (ii): Show that the model (2.3) exhibits Neimark-Sacker bifurcation with the fixed parametric values of $a = 3.71$, $b = 4.8$, $c = 10$, $d = 1$, $e = 10$, $f = 29$, $\beta = 0.5$, and varying values of $\alpha = (0, 0.5]$. We obtained the unique interior positive equilibrium points (H^*, P^*) for the various values of α given in Table 2. At the critical point $\alpha = \alpha_h = 0.4135275$, the model (2.3) has the unique equilibrium point $(H^*, P^*) = (0.357143, 1.56731)$ and the characteristic Eq (2.10) becomes

$$\lambda^2 + 0.538916\lambda + 1 = 0,$$

which shows that $\lambda_1, \lambda_2 = 0.269458 \pm 0.963012i$ are the eigenvalues of (2.9). Then, it satisfies the condition (3.2). It ensures the occurrence of Neimark-Sacker bifurcation near the interior equilibrium point for the model (2.3). Also, for $\alpha = 0.015$, the model (2.3) shows chaotic orbit. Further, for $\alpha = 0.045$, the result is 13-period; for $\alpha = 0.048$, it is 13 invariant circles; for $\alpha = 0.130$, it is 9-period; for $\alpha = 0.410$, it is a closed invariant circle and there is a asymptotically stable equilibrium point at $\alpha = 0.450$. The different nature of the model around the interior equilibrium point for the model (2.3) is shown in the time plots and phase portraits in Figures 4 and 5, correspondingly. The figures show the model undergoes Neimark-Sacker bifurcation. The bifurcation diagram and its largest Lyapunov exponent are shown in Figure 6(a), (b), correspondingly. Since $a^* = -0.151225$ from (3.16), its results are explained in Theorem 3.

In order to show the effect of Allee parameter α on the growth rate parameter a for the values in both Cases (i) and (ii), we have plotted the largest Lyapunov exponents in Figure 7(a),(b). This figures clearly shows the chaotic and stable dynamics of the proposed model.

Table 2. The equilibrium point values for Case (ii).

α	H^*	P^*
0.015	0.357143	2.04886
0.045	0.357143	2.01261
0.048	0.357143	2.00899
0.130	0.357143	1.90991
0.410	0.357143	1.57157
0.450	0.357143	1.52324

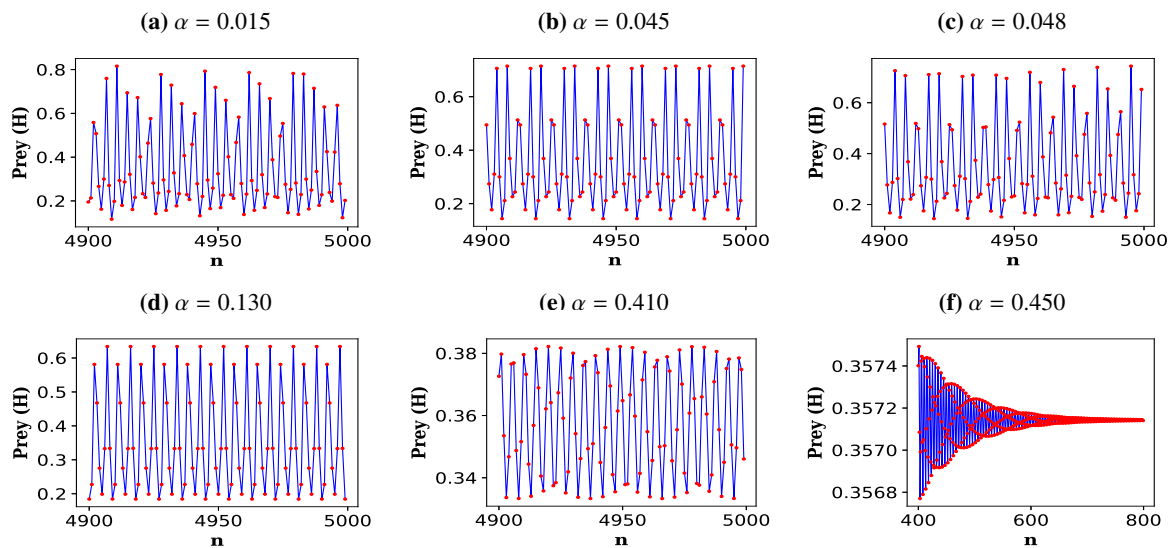


Figure 4. Time-series plots of H_n vs n for the occurrence of Neimark-Sacker bifurcation, where (a) is a chaotic orbit, (b) is period-13, (c) is 13 invariant circles, (d) is period-9, (e) is a closed invariant circle and (f) shows the asymptotically stable non-zero equilibrium point.

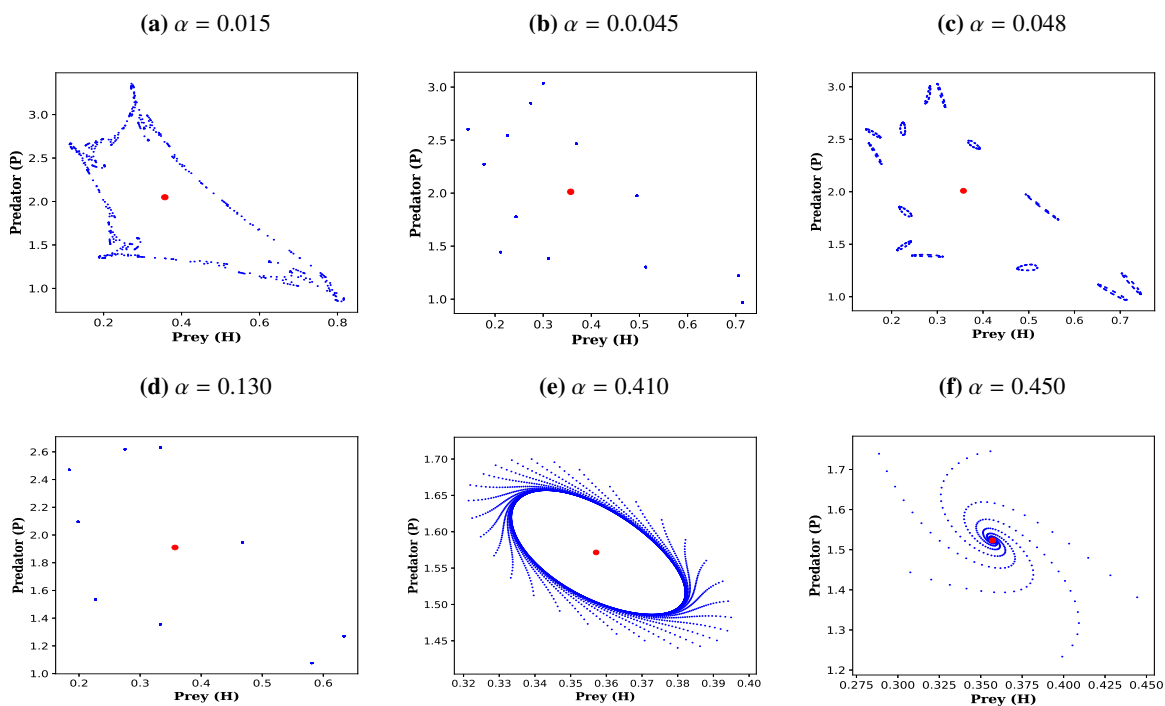


Figure 5. Phase portrait for the occurrence of Neimark-Sacker bifurcation, where (a) is a chaotic orbit, (b) is period-13, (c) is 13 invariant circles, (d) is period-9, (e) is a closed invariant circle and, in (f), asymptotically stable trajectories approach the non-zero equilibrium point. The asterisk symbol represents the unique interior equilibrium point, and its values are given in Table 2.

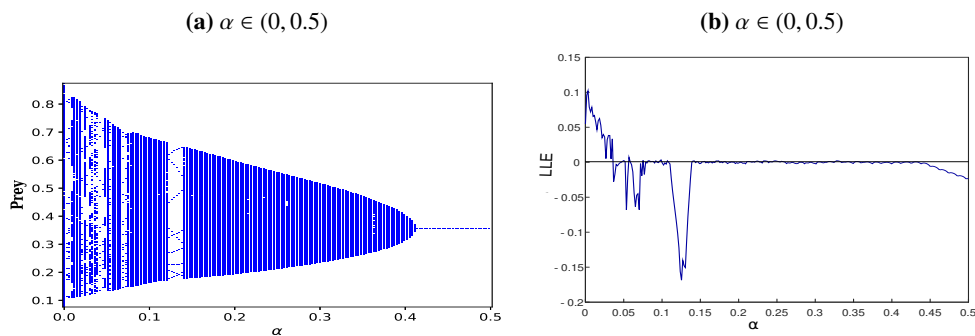


Figure 6. Neimark Sacker bifurcation diagram of the model (2.3) in the (α, H) plane and its largest Lyapunov exponent in (b), correspondingly, with $a = 3.71$, $b = 4.8$, $c = 10$, $d = 1$, $e = 10$, $f = 29$, $\beta = 0.5$, and varying values of $\alpha = (0, 0.5]$.

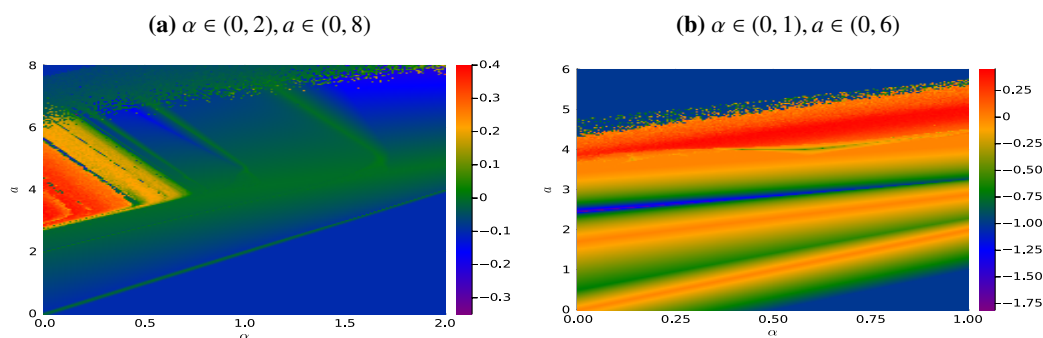


Figure 7. The largest Lyapunov exponents with respect to the parameters in Case (i) as $b = 5.5$, $c = 20$, $d = 0.1$, $e = 10$, $f = 2$, $\beta = 0.5$ and various values of α and a . (b) The largest Lyapunov exponents with respect to the parameters in Case (ii) given $b = 4.8$, $c = 10$, $d = 1$, $e = 10$, $f = 29$, $\beta = 0.5$ and various values of α and a .

5.1. Chaos control

For the particular choice of parameter values $a = 3.71$, $b = 4.8$, $c = 10$, $d = 1$, $e = 10$, $f = 29$, $\beta = 0.5$, and $\alpha = 0.015$, we get the positive unstable equilibrium point $(H^*, P^*) = (0.357143, 2.0488647)$ for the model (2.3) and for its phase portrait (see Figure 5(a)). So, we chose to use the state feedback control method and want to shift the unstable equilibrium point into stable dynamics. For this, taking $\alpha_0 = 0.015$ and the corresponding controlled model yields

$$\begin{cases} H_{n+1} = H_n \exp\left(3.71 - 4.8H_n - \frac{0.015}{0.5+H_n} - \frac{10P_n}{10+H_n}\right) - u(H_n, P_n), \\ P_{n+1} = P_n \exp\left(\frac{29H_n}{10+H_n} - 1\right), \end{cases} \quad (5.1)$$

where $u(H_n, P_n) = h_1(H_n - H^*) + h_2(P_n - P^*)$, and h_1 and h_2 are feedback gains. Furthermore, the Jacobian matrix of the controlled model is given as follows

$$J = \begin{pmatrix} -0.63878 - h_1 & -0.344828 - h_2 \\ 5.539 & 1 \end{pmatrix}.$$

Then, we obtain the characteristic equation as

$$\lambda^2 - (0.36122 - h_1)\lambda + 1.27122 - h_1 + 5.539h_2 = 0.$$

Moreover, the lines of marginal stability for the model (5.1) are computed as

$$L_1 : 0.27122 = h_1 - 5.539h_2, \quad L_2 : 5.539h_2 = -1.91, \quad L_3 : 2h_1 - 5.539h_2 = 2.63244.$$

Then, the triangular region enclosed by the lines L_1, L_2, L_3 has stable eigenvalues for the controlled model (5.1), as shown in Figure 8(a). Clearly, if $h_2 = -0.3$, then $(H^*, P^*) = (0.357143, 2.0488647)$ is locally stable if and only if $h_2 \in [-0.642, 0.4853]$. Taking $h_1 = -0.3$ and $h_2 = 0.3$, then the time-series plots for the controlled model (5.1) are shown in Figure 8(b),(c).

Second, for $a = 3.71, b = 4.8, c = 10, d = 1, e = 10, f = 29, \beta = 0.5$ and $\alpha = 0.015$, the model (2.3) yields $(H^*, P^*) = (0.357143, 2.0488647)$ and its phase portrait is shown in Figure 5(a). So, we chose to use the OGY feedback control method to move the strange chaotic dynamics into the stable dynamics. For this, taking $\alpha = 0.015$ and the corresponding controlled model yields

$$\begin{cases} H_{n+1} = H_n \exp\left(3.71 - 4.8H_n - \frac{0.015 - s_1(H_n - H^*) - s_2(P_n - P^*)}{0.5 + H_n} - \frac{10P_n}{10 + H_n}\right), \\ P_{n+1} = P_n \exp\left(\frac{29H_n}{10 + H_n} - 1\right), \end{cases} \quad (5.2)$$

where s_1 and s_2 are feedback gains. Furthermore, in this case, we have

$$A = \begin{pmatrix} -0.63878 & -0.344828 \\ 5.539 & 1 \end{pmatrix}, \quad B = \begin{pmatrix} -0.416667 \\ 0 \end{pmatrix}, \quad C = \begin{pmatrix} -0.416667 & 0.266158 \\ 0 & -2.30792 \end{pmatrix},$$

and the Jacobian matrix of the controlled model is given as follows

$$A - BK = \begin{pmatrix} -0.63878 + 0.416667s_1 & -0.344828 + 0.416667s_2 \\ 5.539 & 1 \end{pmatrix}.$$

Then we obtain the characteristic equation

$$\lambda^2 + (0.36122 + 0.416667s_1)\lambda + 1.27122 + 0.416667s_1 - 2.30792s_2 = 0.$$

Moreover, the lines of marginal stability for the model (5.2) are computed as

$$\begin{aligned} L_1 : 1.27122 + 0.416667s_1 - 2.30792s_2 &= 1, \\ L_2 : 1.91 &= 2.30792s_2, \\ L_3 : -0.416667s_1 &= 2.63244 + 0.416667s_1 - 2.30792s_2. \end{aligned}$$

Then the triangular region enclosed by the lines L_1, L_2, L_3 has stable eigenvalues for the controlled model (5.2) as shown in Figure 9(a). Clearly, if $s_1 = 0.1$, then $(H^*, P^*) = (0.357143, 2.0488647)$ is locally stable if and only if $s_2 \in [0.55128, 0.82758]$. Taking $s_1 = 0.1$ and $s_2 = 0.7$, then the time-series plots for the controlled model (5.2) are depicted in Figure 9(b),(c).

Finally, we discuss the hybrid control strategy for some parametric values. In this case, the controlled model can be written as

$$\begin{cases} H_{n+1} = \epsilon H_n \exp\left(5.5 - 5.5H_n - \frac{0.20}{0.5 + H_n} - \frac{20P_n}{10 + H_n}\right) + (1 - \epsilon)H_n, \\ P_{n+1} = \epsilon P_n \exp\left(\frac{29H_n}{10 + H_n} - 1\right) + (1 - \epsilon)P_n. \end{cases} \quad (5.3)$$

Moreover, the Jacobian matrix of the model (5.2) at $(H^*, P^*) = (0.526316, 1.26863)$ is given by

$$\begin{bmatrix} 1 - 2.6748\epsilon & -\epsilon \\ 0.228987\epsilon & 1 \end{bmatrix}.$$

The eigenvalues of the above matrix lie inside the open disk if and only if $0 < \epsilon < 0.773477$. For $\epsilon \in (0, 1]$ and $(H^*, P^*) = (0.526316, 1.26863)$, the bifurcation diagram for the controlled model (5.3) are depicted in Figure 10(a),(b).

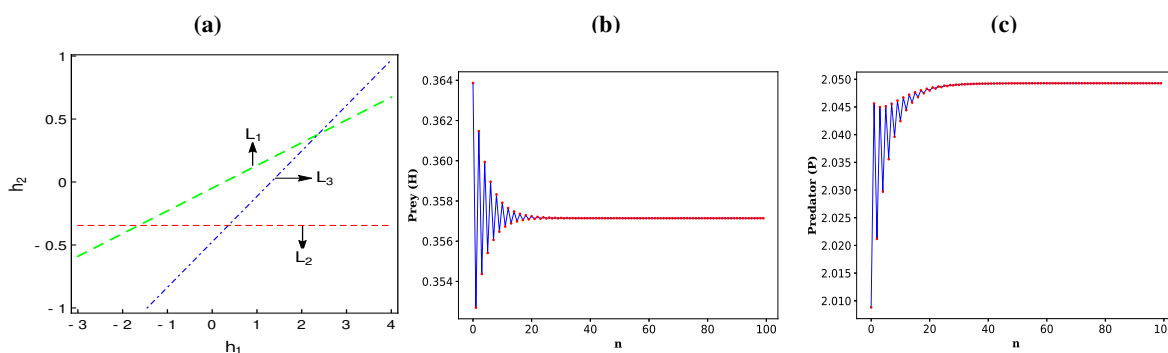


Figure 8. Results for the controlled model (5.1) obtained by the state feedback control method; (a) depicts the stability triangle, (b) and (c) depict the locally stable time series with $h_1 = 0.3$ and $h_2 = -0.3$.

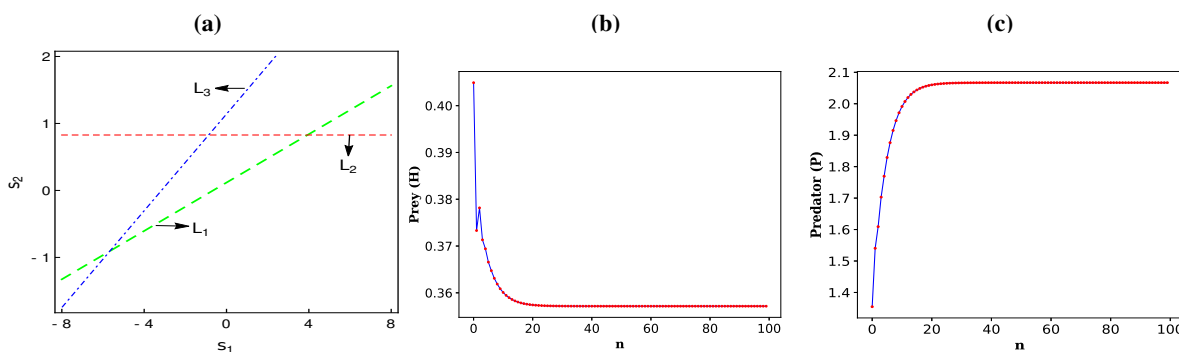


Figure 9. Results for the controlled model (5.2) obtained by the OGY feedback control method; (a) depict stability triangle, and (b) and (c) depicts the locally stable time series with $s_1 = 0.1$ and $s_2 = 0.7$.

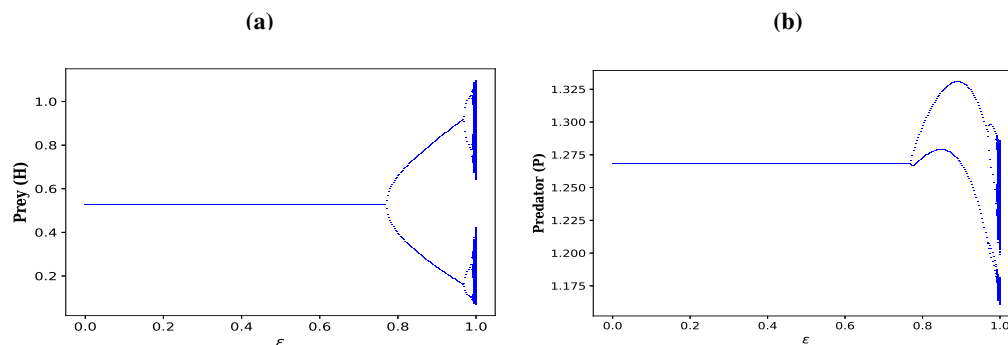


Figure 10. The one parameter bifurcation diagrams for the controlled model (5.3) obtained by the hybrid control method with the control parameter $\epsilon \in (0, 1]$.

Remark 1. *The model (2.3) is the discrete counterpart of the continuous-time model (2.1) investigated in [29]. The method of using a piecewise constant argument for the differential equations has been adopted to obtain the discrete time model, similar to those in [36, 46]. In the absence of predators, the resultant model transforms into the classical Ricker stock recruitment model [37]. It is worth mentioning here that this type of Ricker-type model (2.3) has not been investigated previously. For instance, in [47], the authors studied a basic discrete predator model with the effect of using Ricker map for the prey growth by replacing the classical logistic map; they showed the existence of flip and Neimark-Sacker bifurcations. A Ricker-type predator-prey model with hunting cooperation was investigated by the authors of [48], who studied the existence of discrete Hopf bifurcation. The authors of [29] demonstrated that the model (2.1) experiences Hopf bifurcation, while the model (2.3) undergoes flip and Neimark-Sacker bifurcations and also exhibits chaotic dynamics. The direction and stability properties of both bifurcations can be discussed by using the results from [38, 39]. Also, the bifurcation and chaos control analyses have been carried out using the methods described in [27, 28, 44].*

6. Discussion and conclusions

This paper deals with the discrete-time predator-prey model of Holling II-type interaction with a weak additive Allee effect. In the first step of this study, we derived the discrete-time model from the corresponding continuous model in [29] by using the method of piecewise constant arguments for the differential equations [35]. This discrete form of Lotka-Volterra equations is due to May [9]. The model (2.3) without the Allee effect or predator population has been reduced to a one-dimensional model similar to the model in [37]. The discrete model (2.3) considered in this present work is a good representation of population interaction, as it has a non-overlapping generation, i.e., the birth and death rates occur in certain time intervals. From a biological point of view, the positive equilibrium points for the continuous-time model described in [29] and the discrete-time model (2.3) in this present study are the same, as we showed in Lemma 1. For model (2.3), we showed that the density of the prey population remains unchanged, and that the density of the predator population decreases by increasing the Allee parameter α ; see Tables 1 and 2. The local stability of a coexisting equilibrium (H^*, P^*) is described via Lemma 3, which ensures the long-time survival of both species with the impact of α . In the contrasting continuous-time model [29] of (2.3), for a small value the of Allee parameter,

the model exhibits a periodic solution and becomes locally asymptotically stable via Hopf bifurcation, when the Allee parameter crosses some critical value. Moreover, this is similar to the Neimark-Sacker bifurcation for the discrete model (2.3) in this present study.

Next, we derived the conditions for the existence of flip and Neimark-Sacker bifurcations for model (2.3) around the positive interior equilibrium point by taking the Allee parameter as a bifurcation parameter. We showed the properties of both bifurcations with the help of the CM theorem and normal form theory in Theorems 2 and 3. In the simulation part, we verified all the analytical results numerically. We showed that model (2.3) undergoes flip bifurcation at α_h in Case (i) and Neimark-Sacker bifurcation at α_h in Case (ii), for a different set of parameter values. We notice that model (2.3) has strange dynamics for smaller values of α ; see Figures 2(a) and 5(a). The strange behavior of the model (2.3) for both cases is shown clearly in the one-parameter bifurcation diagrams in Figures 3(a) and 6(a). We notice that the proposed model reduces complex dynamical behavior, and we say that the sensitivity of the population dynamics to initial conditions has been reduced in a sense by the Allee effect. Further, we verified this sensitivity to the initial conditions by plotting the largest Lyapunov exponents in Figures 3(b) and 6(b). In this study, we successfully implemented state and OGY feedback and hybrid control methods by constructing the corresponding controlled models (5.1), (5.2) and (5.3). The lines of stable margins for the controlled models using state feedback control and the OGY feedback control method have been derived and plotted in Figures 8(a) and 9(a). The choice of feedback value inside the stability triangle helps to shift the desired chaotic orbit into the area of stable dynamics, see Figures 8(b),(c) and 9(b),(c). In the case of the hybrid control method, for the control parameter $0 < \epsilon < 0.773477$, the model (5.3) is stable, and the one-parameter bifurcation diagram is shown in Figure 10. A different possibility for showing the existence of chaos in real populations has been provided in the theory of chaos control [26]. The need for this control supports the adoption of the OGY technique for the three fish food chain, i.e., stabilization for the desired periodic orbit. This control condition goes against empirical attempts for lakes and rivers [23].

This study concludes that increasing the Allee parameter, which leads to converting the strange attractor into a proper pattern, i.e., period-16, period-8, period-4, period-2, period-13, period-9 and a closed invariant circle, means that the population oscillates periodically and finally reaches stable dynamics (long-term coexistence of both species) in the considered model. Also, this periodic window and chaotic orbits cannot occur in the counter continuous-time model. This stabilization takes place via both the flip and the Neimark-Sacker bifurcations. In one word, the Allee effect plays a positive role in stabilizing the proposed model, i.e., keeping the population persistent for a long time. However, there will be more complexity in predicting the future population size under chaotic dynamics because a small perturbation in the initial population size can cause massive divergence in population size. For smaller values of the Allee parameter, the presence of bifurcation and chaos in the proposed model can cause both species to have a higher risk of extinction due to unpredictability.

However, it is important to study the discrete-time predator-prey model with the Allee effect in both prey and predator populations. It is interesting to note that one may study the model's relationship to other ecological phenomena like prey refuge, cannibalism and fear impact by appropriately adjusting the strength of the Allee effect simultaneously. Also, considering the other functional responses such as ratio-dependent, Crowley-Martin and Beddington-DeAngelis functional responses, may lead to complex models and cause strange behaviors; we will leave this for future research.

Use of AI tools declaration

The authors declare that they have not used artificial intelligence tools in the creation of this article.

Acknowledgments

This work was partially supported by the Center for Nonlinear Systems, Chennai Institute of Technology, India, with funding number CIT/CNS/2023/RP/016.

Conflict of interest

Prof. Dimplekumar Chalishajar is the Guest Editor of special issue “Recent advances in differential and partial differential equations and its applications” for AIMS Mathematics. Prof. Dimplekumar Chalishajar was not involved in the editorial review or the decision to publish this article.

All authors declare no conflict of interest this paper.

References

1. P. Turchin, *Complex population dynamics*, Princeton University Press, 2013. <https://doi.org/10.1515/9781400847280>
2. R. Arditi, L. R. Ginzburg, Coupling in predator-prey dynamics: Ratio-dependence, *J. Theor. Biol.*, **139** (1989), 311–326. [https://doi.org/10.1016/S0022-5193\(89\)80211-5](https://doi.org/10.1016/S0022-5193(89)80211-5)
3. P. H. Crowley, E. K. Martin, Functional responses and interference within and between year classes of a dragonfly population, *J. N. Am. Benthol. Soc.*, **8** (1989), 211–221. <https://doi.org/10.2307/1467324>
4. J. R. Beddington, Mutual interference between parasites or predators and its effect on searching efficiency, *J. Anim. Ecol.*, 1975, 331–340. <https://doi.org/10.2307/3866>
5. D. L. D. Angelis, R. Goldstein, R. V. O’Neill, A model for tropic interaction, *Ecology*, **56** (1975), 881–892. <https://doi.org/10.2307/1936298>
6. Y. Zhou, W. Sun, Y. Song, Z. Zheng, J. Lu, S. Chen, Hopf bifurcation analysis of a predator-prey model with Holling-II type functional response and a prey refuge, *Nonlinear Dynam.*, **97** (2019), 1439–1450. <https://doi.org/10.1007/s11071-019-05063-w>
7. P. Leslie, J. Gower, The properties of a stochastic model for the predator-prey type of interaction between two species, *Biometrika*, **47** (1960), 219–234. <https://doi.org/10.2307/2333294>
8. H. I. Freedman, *Deterministic mathematical models in population ecology*, Marcel Dekker Incorporated, 1980.
9. R. M. May, Biological populations with nonoverlapping generations: Stable points, stable cycles, and chaos, *Science*, **186** (2007), 645–647. <https://doi.org/10.1126/science.186.4164.64>
10. W. C. Allee, *The social life of animals*, 1938. <https://doi.org/10.5962/bhl.title.7226>
11. F. Courchamp, T. C. Brock, B. Grenfell, Inverse density dependence and the Allee effect, *Trends Ecol. Evol.*, **14** (1999), 405–410. [https://doi.org/10.1016/S0169-5347\(99\)01683-3](https://doi.org/10.1016/S0169-5347(99)01683-3)

12. F. Courchamp, L. Berec, J. Gascoigne, *Allee effects in ecology and conservation*, Oxford University Press, 2008. <https://doi.org/10.1093/acprof:oso/9780198570301.001.0001>
13. B. Dennis, Allee effects: Population growth, critical density, and the chance of extinction, *Nat. Resour. Model.*, **3** (1989), 481–538. <https://doi.org/10.1111/j.1939-7445.1989.tb00119.x>
14. C. E. Brassil, Mean time to extinction of a metapopulation with an Allee effect, *Ecol. Model.*, **143** (2001), 9–16. [https://doi.org/10.1016/S0304-3800\(01\)00351-9](https://doi.org/10.1016/S0304-3800(01)00351-9)
15. C. Celik, O. Duman, Allee effect in a discrete-time predator-prey system, *Chaos Soliton. Fract.*, **40** (2009), 1956–1962. <https://doi.org/10.1016/j.chaos.2007.09.077>
16. W. X. Wang, Y. B. Zhang, C. Z. Liu, Analysis of a discrete-time predator-prey system with Allee effect, *Ecol. Complex.*, **8** (2011), 81–85. <https://doi.org/10.1016/j.ecocom.2010.04.005>
17. N. Iqbal, R. Wu, Y. Karaca, R. Shah, W. Weera, Pattern dynamics and Turing instability induced by self-super-cross-diffusive predator-prey model via amplitude equations, *AIMS Math.*, **8** (2023), 2940–2960. <https://doi.org/10.3934/math.2023153>
18. N. Iqbal, R. Wu, Turing patterns induced by cross-diffusion in a 2D domain with strong Allee effect, *CR. Math.*, **357** (2019), 863–877. <https://doi.org/10.1016/j.crma.2019.10.011>
19. N. Iqbal, R. Wu, W. W. Mohammed, Pattern formation induced by fractional cross-diffusion in a 3-species food chain model with harvesting, *Math. Comput. Simulat.*, **188** (2021), 102–119. <https://doi.org/10.1016/j.matcom.2021.03.041>
20. Z. Chen, Q. Din, M. Rafoqat, U. Saeed, M. B. Ajaz, Discrete-time predator-prey interaction with selective harvesting and predator self-limitation, *J. Math.*, **2020** (2020). <https://doi.org/10.1155/2020/6737098>
21. L. G. Yuan, Q. G. Yang, Bifurcation, invariant curve and hybrid control in a discrete-time predator-prey system, *Appl. Math. Model.*, **39** (2015), 2345–2362. <https://doi.org/10.1016/j.apm.2014.10.040>
22. K. T. Alligood, T. D. Sauer, J. A. Yorke, *Chaos*, Springer, 1996. <https://doi.org/10.1007/b97589>
23. A. Gomes, E. Manica, M. Varriale, Applications of chaos control techniques to a three-species food chain, *Chaos, Solitons & Fractals*, **35** (2008), 432–441. <https://doi.org/10.1016/j.chaos.2006.05.075>
24. R. V. Solé, J. G. Gamarra, M. Ginovart, D. López, Controlling chaos in ecology: From deterministic to individual-based models, *B. Math. Biol.*, **61** (1999), 1187–1207. <https://doi.org/10.1006/bulm.1999.0141>
25. X. S. Luo, G. Chen, B. H. Wang, J. Q. Fang, Hybrid control of period-doubling bifurcation and chaos in discrete nonlinear dynamical systems, *Chaos Soliton. Fract.*, **18** (2013), 775–783. [https://doi.org/10.1016/S0960-0779\(03\)00028-6](https://doi.org/10.1016/S0960-0779(03)00028-6)
26. E. Ott, C. Grebogi, J. A. Yorke, Controlling chaos, *Phys. Rev. Lett.*, **64** (1990), 1196. <https://doi.org/10.1103/PhysRevLett.64.1196>
27. M. S. Shabbir, Q. Din, K. Ahmad, A. Tassaddiq, A. H. Soori, M. A. Khan, Stability, bifurcation, and chaos control of a novel discrete-time model involving Allee effect and cannibalism, *Adv. Differential Equ.*, **2020** (2020), 1–28. <https://doi.org/10.1186/s13662-020-02838-z>

28. Y. Lin, Q. Din, M. Rafaqat, A. A. Elsadany, Y. Zeng, Dynamics and chaos control for a discrete-time Lotka-Volterra model, *IEEE Access*, **8** (2020), 126760–126775. <https://doi.org/10.1109/ACCESS.2020.3008522>
29. Y. Cai, W. Wang, J. Wang, Dynamics of a diffusive predator-prey model with additive Allee effect, *Int. J. Biomath.*, **5** (2012), 1250023. <https://doi.org/10.1142/S1793524511001659>
30. P. Aguirre, E. G. Olivares, E. Saez, Three limit cycles in a Leslie-Gower predator-prey model with additive Allee effect, *SIAM J. Appl. Math.*, **69** (2009), 1244–1262. <https://doi.org/10.1137/070705210>
31. P. Aguirre, E. G. Olivares, E. Saez, Two limit cycles in a Leslie-Gower predator-prey model with additive Allee effect, *Nonlinear Anal.-Real*, **10** (2009), 1401–1416. <https://doi.org/10.1016/j.nonrwa.2008.01.022>
32. S. Vinoth, R. Sivasamy, K. Sathiyathan, G. Rajchakit, P. Hammachukiattikul, R. Vadivel, et al., Dynamical analysis of a delayed food chain model with additive Allee effect, *Adv. Differ. Equ.*, **2021** (2021), 54. <https://doi.org/10.1186/s13662-021-03216-z>
33. M. H. Wang, M. Kot, Speeds of invasion in a model with strong or weak Allee effects, *Math. Biosci.*, **171** (2020), 83–97. [https://doi.org/10.1016/S0025-5564\(01\)00048-7](https://doi.org/10.1016/S0025-5564(01)00048-7)
34. R. E. Mickens, *Nonstandard finite difference models of differential equations*, World Scientific, 1994. <https://doi.org/10.1142/2081>
35. L. Dai, *Nonlinear dynamics of piecewise constant systems and implementation of piecewise constant arguments*, World Scientific, 2008. <https://doi.org/10.1142/6882>
36. S. Vinoth, R. Sivasamy, K. Sathiyathan, B. Unyong, R. Vadivel, N. Gunasekaran, A novel discrete-time Leslie-Gower model with the impact of Allee effect in predator population, *Complexity*, **2022** (2022), 6931354. <https://doi.org/10.1155/2022/6931354>
37. W. E. Ricker, Stock and recruitment, *J. Fish. Boar. Canada*, **11** (1954), 559–623. <https://doi.org/10.1139/f54-039>
38. J. Guckenheimer, P. Holmes, *Nonlinear oscillations, dynamical systems, and bifurcations of vector fields*, Springer Science & Business Media, 2013. <https://doi.org/10.1007/978-1-4612-1140-2>
39. S. Wiggins, *Introduction to applied nonlinear dynamical systems and chaos*, Springer Science & Business Media, 2003. <https://doi.org/10.1007/978-1-4757-4067-7>
40. C. Robinson, *Dynamical systems: Stability, symbolic dynamics, and chaos*, CRC Press, 1998. <https://doi.org/10.1201/9781482227871>
41. R. M. May, G. F. Oster, Bifurcations and dynamic complexity in simple ecological models, *Am. Nat.*, **110** (1976), 573–599. <https://doi.org/10.1086/283092>
42. W. Krawcewicz, T. Rogers, Perfect harmony: The discrete dynamics of cooperation, *J. Math. Biol.*, **28** (1990), 383–410. <https://doi.org/10.1007/BF00178325>
43. G. Chen, X. Dong, *From chaos to order: Methodologies, perspectives and applications*, World Scientific, 1998. <https://doi.org/10.1142/3033>
44. Q. Din, O. A. Gümüş, H. Khalil, Neimark-sacker bifurcation and chaotic behaviour of a modified host-parasitoid model, *Z. Naturforsch. A*, **72** (2017), 25–37. <https://doi.org/10.1515/zna-2016-0335>

45. Y. A. Kuznetsov, *Elements of applied bifurcation theory*, Springer Science & Business Media, 2013. <https://doi.org/10.1007/978-1-4757-3978-7>
46. S. Pal, N. Pal, J. Chattopadhyay, Hunting cooperation in a discrete-time predator-prey system, *Int. J. Bifurcat. Chaos*, **28** (2018), 1850083. <https://doi.org/10.1142/S0218127418500839>
47. M. Y. Hamada, T. E. Azab, H. E. Metwally, Bifurcations and dynamics of a discrete predator-prey model of ricker type, *J. Appl. Math. Comput.*, **69** (2023), 113–135. <https://doi.org/10.1007/s12190-022-01737-8>
48. Y. H. Chou, Y. Chow, X. Hu, S. R. J. Jang, A Ricker-type predator-prey system with hunting cooperation in discrete time, *Math. Comput. Simulat.*, **190** (2021), 570–586. <https://doi.org/10.1016/j.matcom.2021.06.003>



AIMS Press

©2023 the Author(s), licensee AIMS Press. This is an open access article distributed under the terms of the Creative Commons Attribution License (<http://creativecommons.org/licenses/by/4.0>)